CODEN:LUTEDX/(TEIE-5283)/1-60(2011)

Industrial Electrical Engineering and Automation

Deriving and Implementing a Model of the Fifth Generation Haldex AWD Actuator

Jonas Berge
David Berggren

Division of Industrial Electrical Engineering and Automation
Faculty of Engineering, Lund University

Deriving and Implementing a Model of the Fifth Generation Haldex AWD Actuator

Jonas Berge and David Berggren

Abstract

The objective for this master thesis has been to develop a mathematical model of the actuator parts of the fifth generation Haldex AWD system. The parts to be modeled are the DC-Machine and the pump. Also a model of the elasticity of the clutch has to be derived as well as a model for the hydraulic fluid. These models were then to be implemented in Matlab Simulink.

The model was derived by means of standard modeling. That is, by studies of the mechanical subparts, use of equilibrium equations and their relations to each other.

To evaluate the model the simulated flow of the pump, the viscosity of the fluid and pressure of the pump was compared to results measured on the actual hardware. These comparisons showed that the model is a good approximation of the actual hardware.

Sammanfattning

Målet för detta examensarbete var att utveckla en matematisk modell av de drivande delarna i den femte generationen Haldex AWD-system. De delarna är DC-maskinen och pumpen. Även en modell av elasticiteten i kopplingen skulle härledas liksom en modell för hydrauloljan. Dessa modeller skulle därefter implementeras i Matlab Simulink.

Modellen utvecklades med modelleringsmetodik. Det vill säga att den härleddes genom studier av de mekaniska delarna, genom friläggning av dessa samt uppställning av jämviktsekvationer.

För att utvärdera modellen simulerades flödet av pumpen, viskositeten på vätskan och trycket i pumpen. Dessa jämfördes med resultaten uppmätta på det verkliga systemet. Dessa jämförelser visade att modellen är en bra uppskattning av den verkliga hårdvaran.

Content

Preface

This Master's thesis was carried out at Haldex Traction AB in Landskrona in cooperation with the *Division of Industrial Electrical Engineering and Automation* and the *Department of Automatic Control* at the Faculty of Engineering at Lund University. The thesis will be published in each of these departments.

Most of this work is a close collaboration between the authors and has been worked on at the same degree by both. But the modelling is one area where they divided the work between them. Jonas Berge has worked on the hydraulic fluid, the clutch and the models of them, while David Berggren has worked on the flow dynamics through the pump and the lever arms. The other derivations, such as DC motor, piston dynamics and the load torque has been a collaboration between the authors. Similarly, the report has been processed to the same extent by both authors.

The objective was to implement a Matlab/Simulink model of the system hardware to use as a supporting tool in the development of the control system.

First of all we would like to thank Haldex Traction for giving us the opportunity to be a part of the development process of the generation V AWD system. Secondly we would like to thank our supervisors, Johan Nilsson at Haldex Traction, Bengt Simonsson at the *Division of Industrial Electrical Engineering and Automation* and Rolf Johansson at the *Department Automatic Control* for their help and support.

Moreover many thanks go to Pierre Petterson and Måns Ranåker at Haldex Traction whom always took the time to answer questions and guide us.

It is assumed that the reader of this thesis possesses good knowledge in mechanical and electrical engineering.

Landskrona January 2011

David Berggren and Jonas Berge

Terminology

AWD	All wheel drive. A vehicle equipped with a drive train allowing all four wheels to receive torque from the engine. Can be partly or permanent.
LSC	Limited slip coupling. Distributes torque between the front and rear axis.
ECU	Electronic control unit. Contains the software and control algorithms for the AWD system
PMDC machine	Permanent magnetized direct current machine
Swash plate	Determines the displacement of the pump. In this case the swash plate is actually an angled thrust bearing but will from here on be referred to as swash plate.
TDC	Top dead center.
BDC	Bottom dead center.
CoG	Center of Gravity.
ABS	Anti-lock Breaking System
ESP	Electrical Stability Program

1 Introduction

1.1 Background

When driving under demanding conditions such as snow, ice and mud, a regular two wheel driven car will fall short. To increase safety and performance many car manufacturers offers a four wheel driven alternative. However there are a vast variety of four-wheel drive setups. Some systems are full-time AWD, which means that all wheels receive torque from the engine at all time. The amount of torque distributed between the front and rear axis can have a fixed ratio, typically 50/50 or be variable. These kinds of full time systems are common amongst the Asian car manufacturers such as Subaru and Toyota.

As an alternative to the full time systems there are systems called part time. Cars using a part time system can either be front or back wheel driven under normal driving conditions. To distribute torque to the other axis some kind of torque transferring device is needed (see *Figure 1.1*). There are a variety of different solutions how this can be achieved. To transfer torque between the right and left wheels, a differential able to split the available torque is needed.

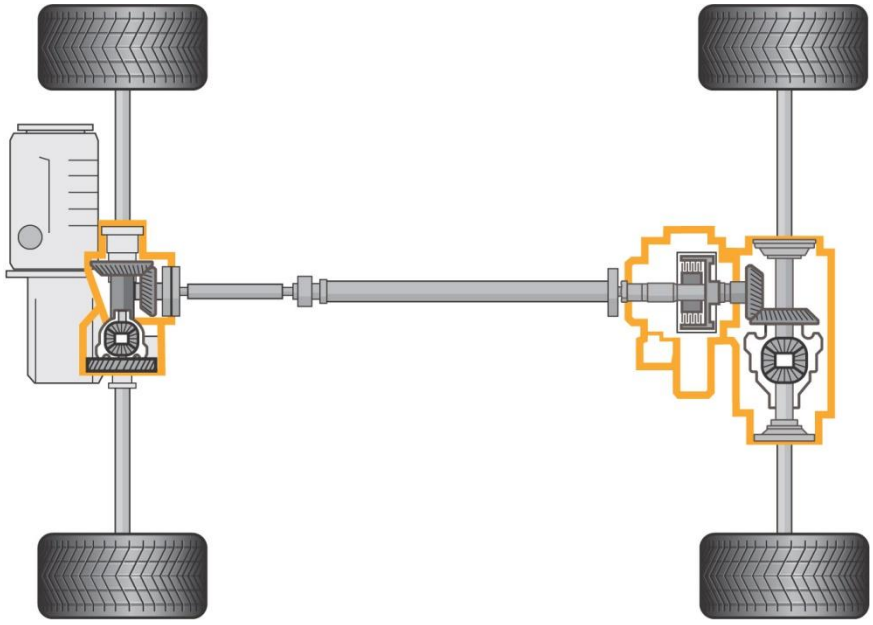

Figure 1.1 Illustration of the driveline. Highlighted areas are the rear and forward differentials and the AWD coupling.

On modern cars, these systems are usually integrated with other systems such as ABS and ESP. These systems receive data from a number of onboard sensors. In case the vehicle starts to slip the system automatically engages and helps the driver to stabilize the vehicle.

Apart from increasing the safety one of the benefits of a part time system is slightly reduced fuel consumption due to reduced losses in the drive train. On the other hand a part time system is harder to control and often suffers from delay. It needs a

fast and reliable control strategy to prevent the system from causing unexpected behavior.

In development of such algorithms a model of the system is of great use. Time and money can be saved when the necessity of testing the software directly on the system is decreased.

1.2 Company history

The Haldex concern [1] was created in 1985 by merging three Swedish companies: Garphyttan, Haldex and Hesselman. At that time the main source of revenue was the spring wire industry with 50 percent of the total sales. However, the division was sold in 2009 and the departments Traction and Hydraulic now generate the main revenue.

With the acquisition of Barnes Corp in 1987 and Vickers in 1991 the hydraulics section of the concern was built up. A patent for a new four-wheel drive was bought in 1992. The first generation clutch was marketed in 1998. This was also the year Haldex Traction Systems was created as a division of the Haldex concern.

1.3 Haldex Traction Systems

The patent Haldex acquired in 1992 was bought from former rally driver Sigge Johansson [1]. The main idea was for the clutch to be actuated by a pump driven by the difference in rotational velocity of the wheels. Haldex developed the clutch in a close cooperation with Volkswagen. In 1998 the series production of the 1st generation clutch commenced.

A long series of companies have since then used the clutch in their cars, among others Volvo, Ford, Bugatti and SAAB/GM [2]. The clutch has since 1998 been developed further and the fifth generation is now under development. In 2009 Haldex announced a deal with Volkswagen worth SEK 4.5 billion to provide their next platform with this, fifth generation system.

1.4 Previous generations

The first two generations AWD are quite similar and are actuated by a difference in wheel speed. This movement drives a hydraulic pump, which generates flow and actuates the LSC. This means that these systems are reactive i.e. a wheel slip needs to occur before the system is engaged. 1/4 revolution of the wheel generates enough flow to completely lock the axis. The pressure level in the LSC is controlled by the ECU and regulated by a linear throttle valve.

Generation II is a further development of the first generation but with more sensors and a solenoid proportional valve, the overall performance was increased.

To further reduce the response time Haldex introduced generation III with pretension capabilities, PreX. Adding a small feeder pump, making it possible to provide torque to the rear wheels, even though no wheel spin has occurred, reduced the response time. By adding this feature the system is now proactive meaning that the system is able to adjust the need of AWD in real time based on information provided by the onboard sensors.

1.5 Generation IV

With the Haldex generation IV a unique all-wheel drive system was introduced. The system is described as intelligent and able to sense the driver's intentions. The torque is at all times divided among the four wheels. However, the distribution can be as low as 2% of the total and as high as 85% on a single rear wheel.

By transmitting only 4% of the torque to the rear axis during cruising, energy consumption is reduced. And if slip occurs on three tires at the same time, as much of the available torque as possible is transferred to the tire that is having grip.

This distribution between the rear wheels is controlled by a multiplate clutch (see *Figure 1.2*), regulated with hydraulic pressure. Earlier generations of this had complaints about lagging response times. This was due to not being able to accumulate pressure fast enough. By introducing an accumulator (see *Figure 1.2*) with a separate feeder pump a high pressure could be instantly available to use for control. This control is executed by the Electrical Control unit (ECU). By using more than 20 sensors around the car the ECU updates the torque distribution 100 times a second.

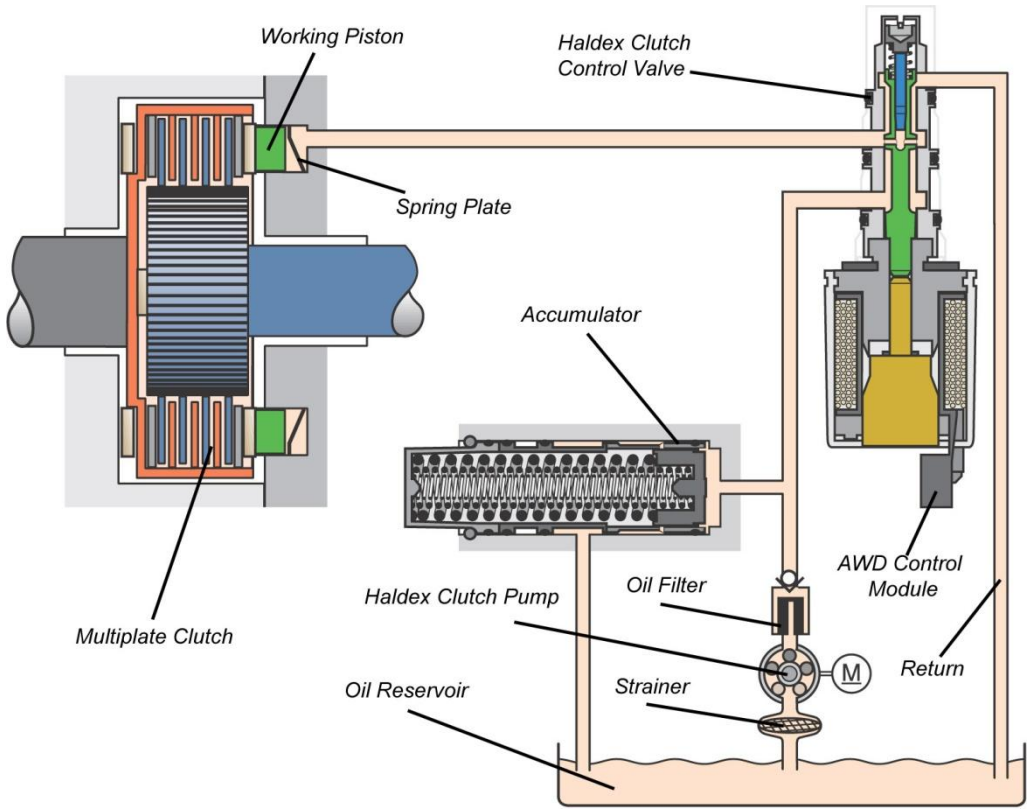

Figure 1.2 Schematics of the actuator parts in the fourth generation system (Source: [2]).

1.6 Gen V

To reduce weight and space the accumulator and the control valve added to the fourth generation coupling are now removed (see *Figure 1.3*). Instead the pressure shall be generated directly to the clutch pack using a specially designed feeder pump.

A pump is a flow-generating machine, the medium flowing in this case being hydraulic oil. The pressure on the clutch pack is generated when the oil is pumped in to the chamber containing the piston that transfers this pressure to the plates.

To keep the response times sufficiently low the pump has a design where the flow of fluid has two different paths it can be guided through. When a steady state of pressure is reached no more fluid is flowing into the clutch, only being pumped out to the surrounding system. When an increase in pressure is requested the way out is shut and the entire flow is going into the clutch pack.

2 Problem Formulation

2.1 Objectives

The objectives of this thesis are to create a model of the AWD clutch actuator system. The system subparts to be modeled is a DC motor, an axial hydraulic pump, a model for the elasticity of the clutch and the hydraulic fluid. The main objective for Haldex are to be able to run simulations using the model and pre-existing functions for the control of the clutch, thereby saving time in development process.

The model should account for different ambient- and hydraulic fluid temperatures. This shall be implemented in MATLAB/Simulink.

2.2 Delimitations

DC machine

- The model shall be as general as possible, making it possible for Haldex to use it for different motors, in future projects.
- The parameters supplied from the manufacturer are assumed to be correct.
- Eddy currents and armature reactions will not be included in the model.
- Assumes a rigid connection via the axis to the pump.

Pump

- Will be modeled as general as possible for the same reasons as stated above.
- Forces from friction due to centripetal acceleration and earth gravity will not be considered.
- Losses in pressure, such as channel losses and other minor losses, too small to be of consequence will be neglected.

Hydraulic fluid

- Will be modeled using data provided by Haldex, data assumed to be correct.
- The viscosity and density will be approximated as a function of temperature i.e. the influence of pressure will be neglected.
- Effects of air mixture in the fluid will be neglected.

Complete Model

- Built according to Haldex modeling guidelines for MATLAB/Simulink models.

2.3 Simulation software

Simulink is a software package inside MATLAB used for modeling and simulation of dynamical systems [3]. Both linear and nonlinear systems can be simulated in continuous time, sampled time or a hybrid of both using different solvers.

Simulink uses a graphical interface for building models as block diagrams. The Simulink library contains many pre-defined blocks common to modeling and can be extended with user customized function blocks. The blocks are then simply

connected with wires. To make the model easy to overview and manage, different functions of the model can be placed into different subsystems.

The simulations can be viewed and analyzed in real time by connecting scopes to the signals of interest. Simulation data can also be exported and stored in the MATLAB workspace.

2.4 Outline of the Thesis

This system has three major sub parts, the dc motor, the hydraulic pump and the hydraulic fluid as well as one minor part; the clutch elasticity. The first chapters of this thesis cover the underlying theories followed by the derived model for each subsystem. Each subsystem will be evaluated before it is merged into a complete system. The thesis finishes with discussion and conclusion.

3 Theory and Modeling

The complete model will consist of four subsystems, the motor, pump, oil and the multiplate clutch. In *Figure 3.1* a modified version of the original schematic (see *Figure 1.2*) can be viewed, illustrating the Gen V system. The first system will be the electrical motor. The signals in to this subsystem are the armature voltage and the temperature. These signals also are the signals into the complete model. Output from the motor subsystem is the armature current and the motor axis dynamics, i.e. the rotational velocity, acceleration of the axis and position.

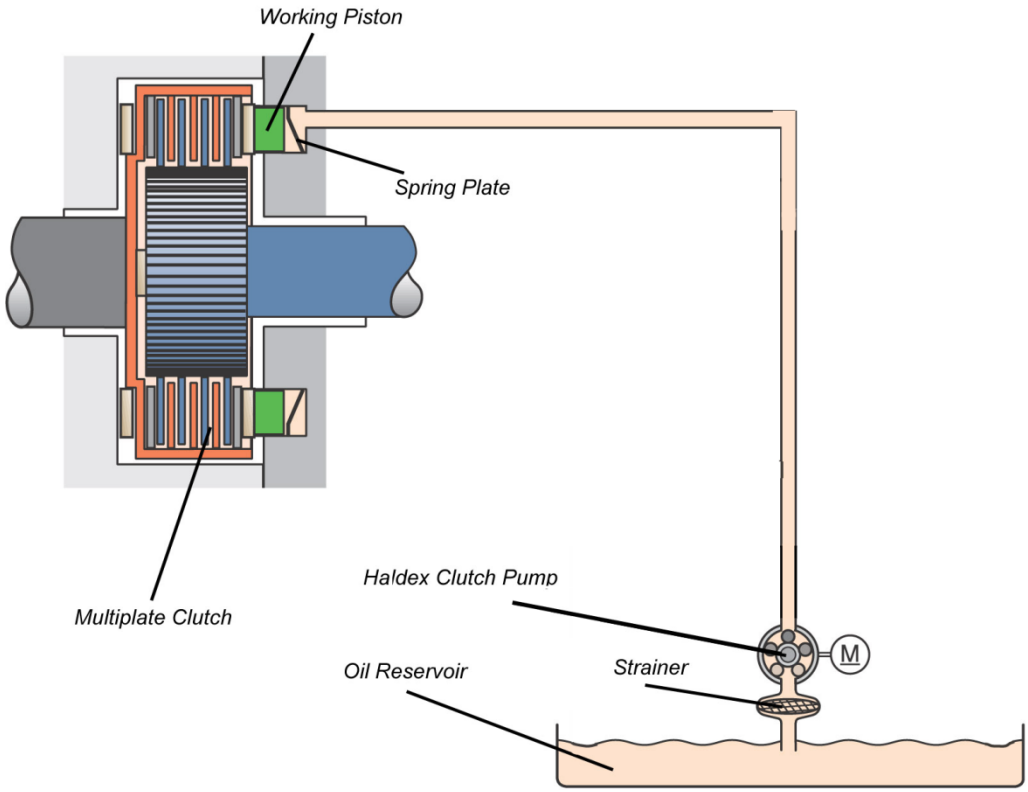

Figure 3.1 Schematics of the Gen. V Haldex coupling (Source: [2]).

The motor axis dynamics is input to the pump subsystem together with the oil dynamics and clutch pressure. Output from the pump is the net flow in or out of the pump. This flow is the input of the clutch model, which has the clutch pressure as output. This pressure is then fed back to the pump. The subsystem that calculates the dynamics of the oil has temperature as input and is then connected to the pump. The output from the complete model is the clutch pressure and the armature current. A block diagram that illustrates this can be viewed in *Figure 3.2.*

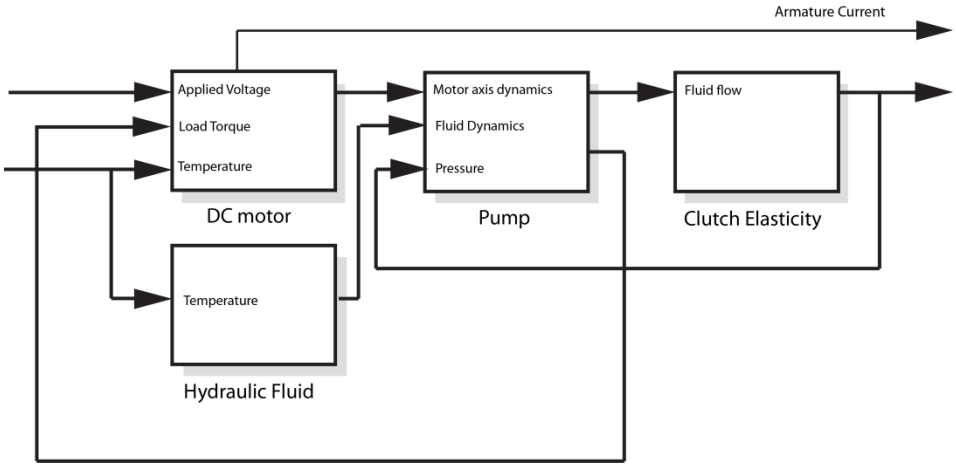

Figure 3.2 Block diagram of the complete models subsystems.

3.1 DC machine

3.1.1 Introduction

The DC machine is frequently used as an actuator throughout industry today. The fundamental design of the machine makes it sturdy and less likely to malfunction or break down during operation. It also has an almost linear armature voltage and speed relation as well as an almost linear current and torque relation, making it relatively easy to control.

This chapter will cover the actuator for the pump of the gen. V AWD system. Firstly there will be a short description of the working principle of the DC machine followed by an overview of the motor equations.

The gen. V motor is a 12-pole permanent magnetized DC machine. Since there is no actual runtime data available the standard motor equations will be used to model the motor. Some additions will be made regarding different kinds of friction. The model implemented in Simulink also accounts for different kinds of ambient temperature. The manufacturer provided the data for this.

3.1.2 Working principle

A PMDC motor consists of rotor-mounted windings, a number of north and south pole magnets arranged in pairs, and a commutator [4]. The permanent magnets are mounted around the stator (see *Figure 3.3*). The commutator is a set of copper conductors mounted to the rotor. Current is passed to the commutator via a pair of carbon brushes, which slide along the commutator surface when the rotor rotates.

When the brushes change plate the current in the coils changes direction. Since the current in the coil creates a magnetic field, this change in current direction also changes the polarity of that magnetic field. By placing the coils and commutators, such that the induced magnet field either attracts or repels the magnets in the stator, a torque is created.

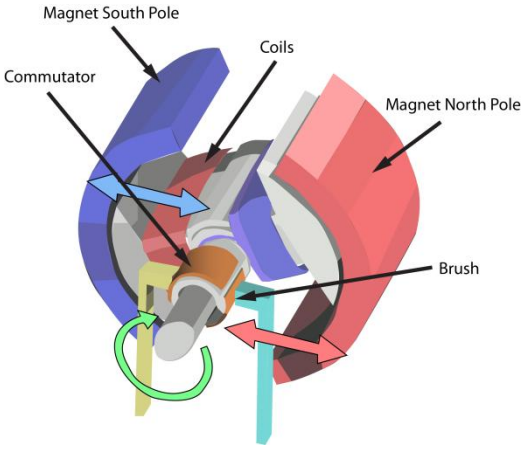

Figure 3.3 PMDC machine.

3.1.3 Governing equations

The circuit that represents the DC motor is illustrated in its schematic form in *Figure 3.5*. The differential equations [4] describe the armature current, i_a, the induced voltage in the armature, u_a, and the electrical torque, m_d. The equations are

$$R_a i_a + L_a \frac{di_a}{dt} + e = u_a \tag{3.1}$$

$$e = c_1 \Phi_e \omega \tag{3.2}$$

$$J \frac{d\omega}{dt} = m_d - m_L \tag{3.3}$$

$$m_d = c_2 \Phi_e i_a \tag{3.4}$$

$$\Phi_e = f(i_e) \tag{3.5}$$

where m_L is the load torque on the motor axis. This model is one of a separately exited DC machine and therefore also includes a function for the electrical magnetic flux, Φ_e. Since the motor in Gen V is a PMDC motor, equation

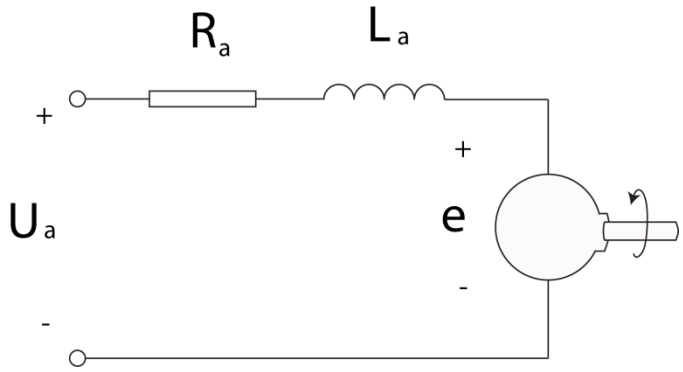

Figure 3.5 Schematics of the DC-machine.

(3.2) and (3.3) can be further simplified. This is because the permanent magnet's magnetic flux is considered to be constant [5]. The equation (3.4) is thus simplified to:

$$m_d = \Psi_m i_a \tag{3.6}$$

By introducing Ψ_m as the magnetic flux and rearranging (3.1), the final current equation is reached:

$$\frac{d i_a}{d t} = -\frac{R_a}{L_a} i_a - \frac{c_1}{L_a} \Phi_e \omega_m + \frac{1}{L_a} u_a \tag{3.7}$$

3.1.4 Solution DC Machine

The manufacturer of the DC motor has provided temperature dependent data and constants for the motor. The relevant constants are the torque constant *kT*, and the voltage constant *kE.*

$$m_d = c_1 \psi_m i_a = k T i_a \tag{3.8}$$

$$e = c_2 \Phi_e \omega = kE\omega \tag{3.9}$$

3.1.5 Friction and losses

The equations presented in the previous chapter do not include any losses in the motor. There are two types of friction losses [4] occurring there; viscous damping and dynamic friction torque. Both of these are temperature dependent. The viscous damping is a friction torque caused by lubrication liquid and moving parts in the motor and is considered directly proportional to the speed. The dynamic friction torque is the Coulomb friction and is considered a constant term adding to the losses.

Adding these terms to (3.3) and introducing new notations the final torque equation is obtained:

$$J \frac{D\omega}{dt} = m_d - m_L - m_{Fi} - m_{Tfd} \tag{3.10}$$

$$m_{Fi} = c_3 \omega = F_i \omega \tag{3.11}$$

$$m_{Tfd} = c_4 = Tfd \tag{3.12}$$

Where m_{Fi} is the viscous damping and m_{Tfd} is the dynamic friction torque.

Other phenomena like eddy currents and field weakening will also cause losses. Eddy currents arise when a conductor is exposed to a change in magnetic flux [5]. This can cause a current to circulate within the conductor. These circulating currents create a magnetic field that opposes the magnetic flux from by the permanent magnet.

Field weakening occurs when current is flowing through the coil windings. The current creates a magnetic field that distorts and weakens the field in the same way that eddy currents do. Due to lack of experimental data the influence of these phenomena will be neglected.

3.1.6 Final Motor Equations

Using the equations (3.11), (3.12) and new notations the governing equations for the DC machine is obtained

$$J\frac{d\omega}{dt} = kTi_a - m_L - F_i\omega - Tfd \tag{3.13}$$

$$\frac{di_a}{dt} = -\frac{R_t}{L}i_a - \frac{kE}{L}\omega + \frac{1}{L}u_a \tag{3.14}$$

where R_t, kE and kT are temperature dependent parameters.

3.1.7 Simulink Model

The motor block in the Simulink model has three inputs: the armature voltage *u_a,* the load from the pump *T_load* and the motor temperature *Temp.* The last input is affect the temperature dependent parameters earlier mentioned. Inside the block, a lookup table is used for each of these parameters using *Temp* as an input.

The outputs from the block are the armature current, the effective load torque generated by the machine and both the rotational velocity and the angular position of the shaft. See Appendix A for further information.

3.2 Hydraulic pump

3.2.1 Introduction

An axial piston pump consists of three main components, the barrel containing the pistons, the pump lid and the swash plate [6]. The angle of the swash plate determines the pump displacement and can be variable or fixed. On the Gen V. pump the swash plate is an angled thrust bearing with a fixed angle. The barrel is held against the pump lid, which contains the suction and discharge ports. The arrangements of these ports are such that the suction port is connected to the low-pressure side of the system, and the discharge port to the high-pressure side. When the barrel rotates, the pistons slide along the swash plate. The angle of the swash plate forces the pistons to reciprocate back and forth which creates the pumping action, i.e. sucking fluid from the low-pressure side, discharging it at the high-pressure side.

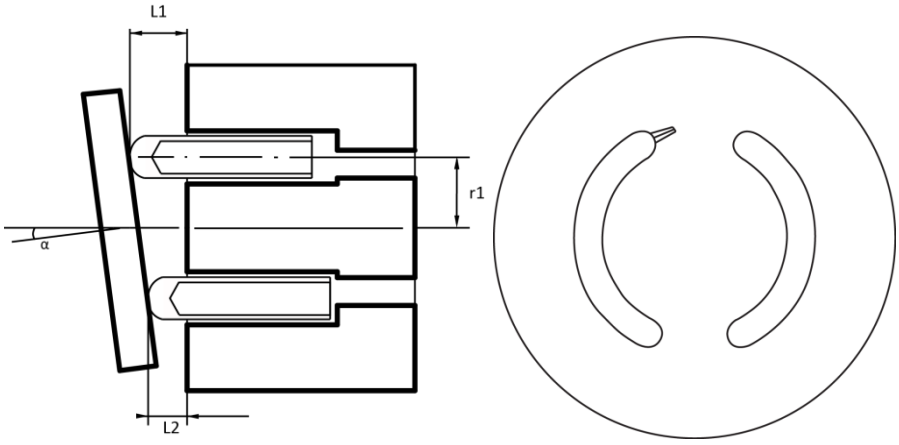

Figure 3.6 Cross section of the swash plate, barrel, pistons and pump lid.

In *Figure 3.6* there is a crosscut of the barrel, pistons, swash plate and the pump lid. The governing properties for the pump capacity are the swash plate angle and the rotational velocity.

As mentioned in the introduction, a pump is a flow-generating machine. This flow generates a pressure in the clutch chamber. As soon as the desired pressure is reached at the clutch the flow generated by the pump needs an alternative route else it would continue to build up pressure.

The centre of the Gen V pump barrel is hollow and the pressurized fluid is allowed to reach this chamber. From this chamber, three drilled channels lead the fluid to the surface of the barrel. At the surface there are three arms, levers, rotating with the barrel. They are designed to control the opening and closing of the channel orifices.

If the rotational velocity is high enough the centripetal force pivots the arm and pushes a ball located at its shorter end into the outlet, thereby closing it shut (see *Figure 3.7*). When the pressure in the chamber rises, the force from the fluid causes a pivoting action in the opposing direction from the centrifugal force. This opens the outlet and allows for flow out to the surrounding system.

The arms also act as a check valve when the pumping actions stops, the high built up pressure in the system will lift the arms and thereby create a high flow through the channel orifices and cause a quick pressure drop.

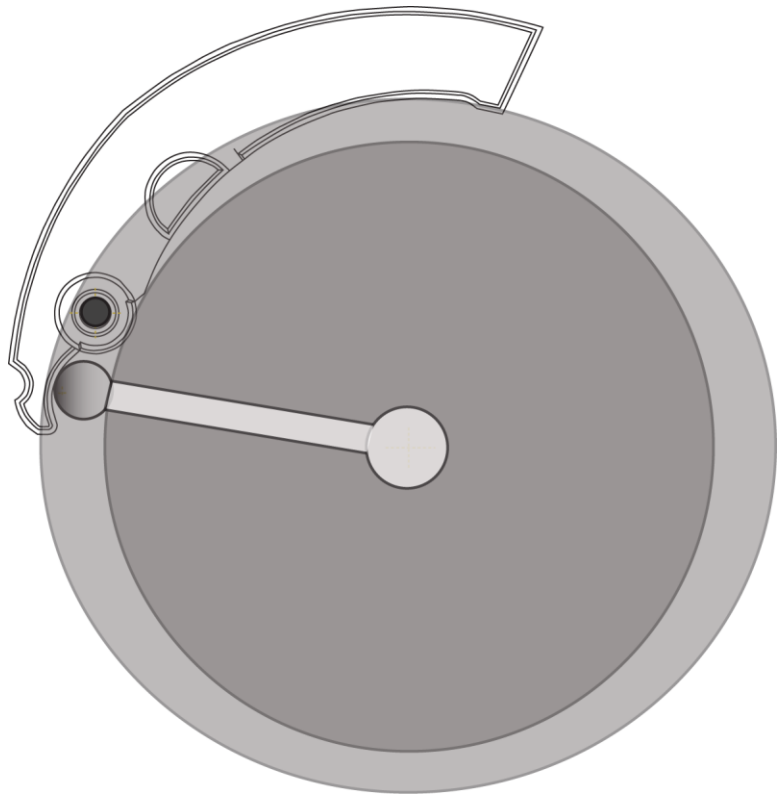

Figure 3.7 Barrel, arm and flow outlet.

3.2.2 Piston position

To accurately account for the forces operating on the piston a coordinate system for the pump barrel, swash plate and piston position needs to be established. The defined x-, y, z-plane has its x-axis in the shaft direction of the dc-machine. The coordinate system is illustrated in *Figure 3.8.*

By study the schematics the axial position of the piston can be determined by:

$$x_p(\theta) = -r_1 \tan(\alpha)\sin(\theta) + pos\_adj \tag{3.15}$$

where r_1 is the radius to the centre of the barrel to the pistons, and α the angle of the swash plate. This gives a position that is oscillating between a positive and negative value. The constant *pos_adj,* is then added to balance the position to be equal to zero at BDC. Since the speed and acceleration will be needed to calculate the forces upon the piston this is derived.

$$\dot{x}_p(\theta) = -r_1 \tan(\alpha)\cos(\theta)\dot{\theta} = -r_1 \tan(\alpha)\cos(\theta)\omega \tag{3.16}$$

$$\ddot{x}_p(\theta) = r_1 \tan(\alpha)\sin(\theta)\dot{\theta}^2 = r_1 \tan(\alpha)\sin(\theta)\omega^2 \tag{3.17}$$

The y-, and z-coordinates are simply

$$y_p(\theta) = r_1 \cos(\theta) \tag{3.18}$$

$$z_p(\theta) = r_1 \sin(\theta) \tag{3.19}$$

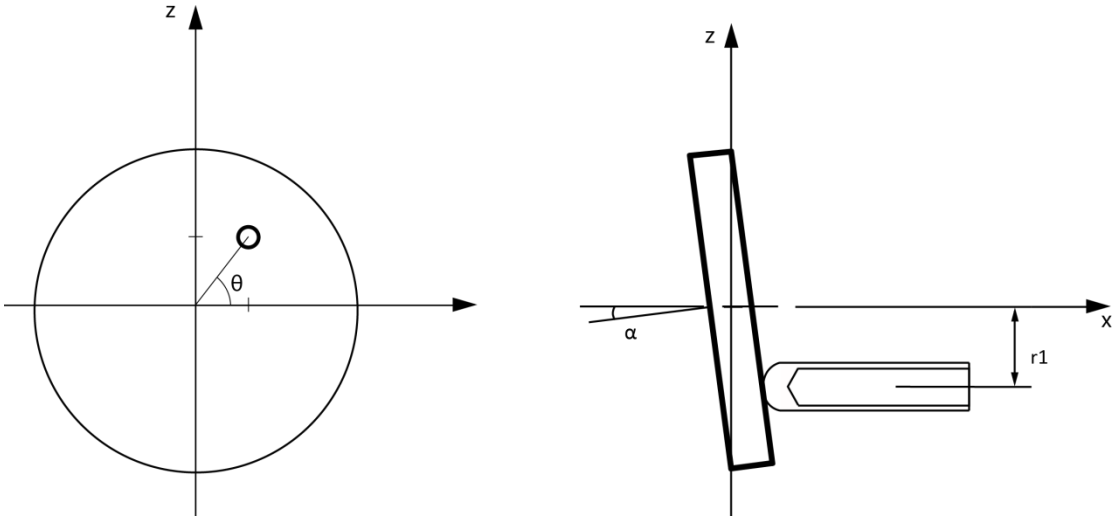

Figure 3.8 Coordinate system of the piston and swash plate.

3.2.3 Piston Forces

By making an equilibrium equation of the system the forces acting on it can be determined. In *Figure 3.9* the forces acting on one piston in the x-direction is illustrated. The equilibrium equation in the x-direction is established

$$\ddot{x}_p(\theta)m_p + F_s\cos(\alpha) = F_f + F_k + p_p \cdot A_p \tag{3.20}$$

The friction force due to viscosity in the cylincer when a piston is moving within is determined by the following equation [6]. The main parameters governing this equation are the viscosity, η, the mean clearance between the piston and the cylinder, h_0 and the piston velocity, $\dot{x}_p$.

$$F_f = \frac{2\pi r \eta \dot{x}_p(\theta) l_p}{h_0\sqrt{1-\left(\frac{e}{h_0}\right)^2}} - \pi r h_0 \Delta p \tag{3.21}$$

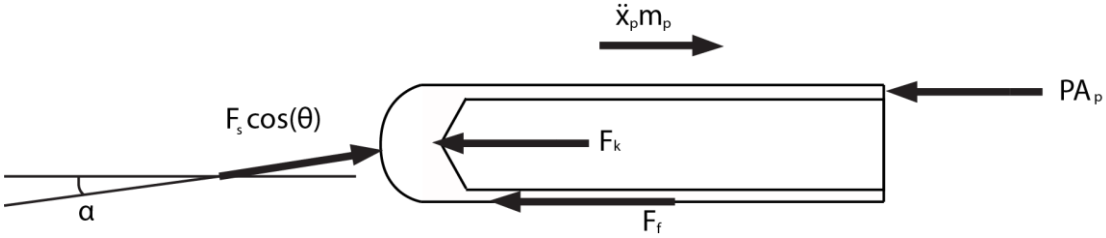

Figure 3.9 Forces acting on the piston in the x-direction.

The forces in the z-direction can be calculated as a function of the axial angle. It is assumed that the reaction forces from the barrel on the piston are located on the inner most area of the piston and the point where the piston leaves the barrel. This is illustrated in *Figure 3.10.* By making an equilibrium equation of the piston a moment equation can be established.

$$F_s\sin(\alpha)(c_1 + x_p(\theta)) = F_{t2}(l_p - (c_1 + x_p(\theta))) \tag{3.22}$$

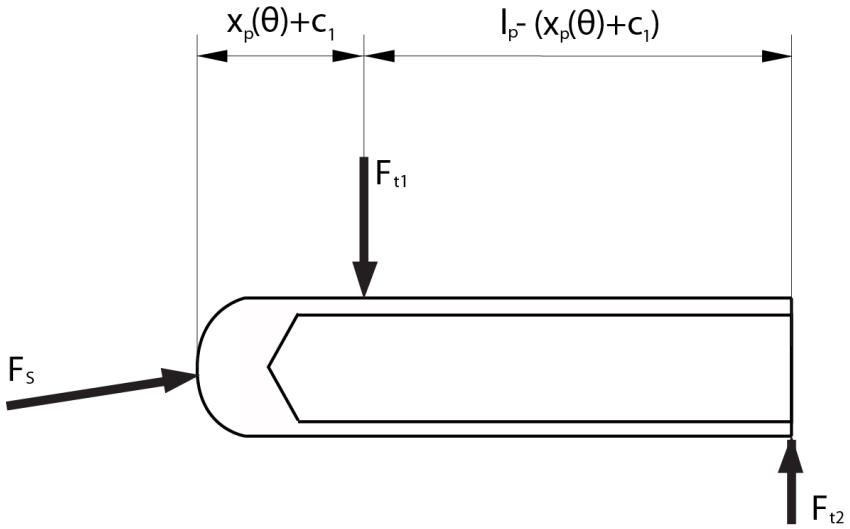

Figure 3.10 The forces acting on a piston in the z-direction.

which gives

$$F_{t2} = \frac{F_s \sin(\alpha)(c_1 + x_p(\theta))}{(l_p - (c_1 + x_p(\theta)))} \tag{3.23}$$

$$F_{t1} = F_s \sin(\alpha)\left(1 + \frac{(c_1 + x_p(\theta))}{(l_p - (c_1 + x_p(\theta)))}\right) \tag{3.24}$$

These forces, F_{t1} and F_{t2} will be used to calculate the losses due to friction in the piston chamber.

The equation for the spring force is

$$F_k = k_p x_p(\theta) + c_k \tag{3.25}$$

After rearranging the equation (3.20) an expression for the force acting on the swash plate is obtained

$$F_s = \frac{P_p A_p - \ddot{x}_p(\theta) m_p + F_f + F_k}{\cos(\alpha)} \tag{3.26}$$

3.2.4 Lever Arm

The goal with this section is to calculate the flow out through the opening at the arms. This flow is governed by the area of the orifice at the end of the channel. This area in turn is governed by Δy_1, which is the elevation between the orifice and the ball at the end of the lever arm. The equilibrium equation for the arm is illustrated by *Figure 3.11* and with the pin hole as rotational centre is given by

$$F_p l_1 + F_k l_2 = F_m l_3 \tag{3.27}$$

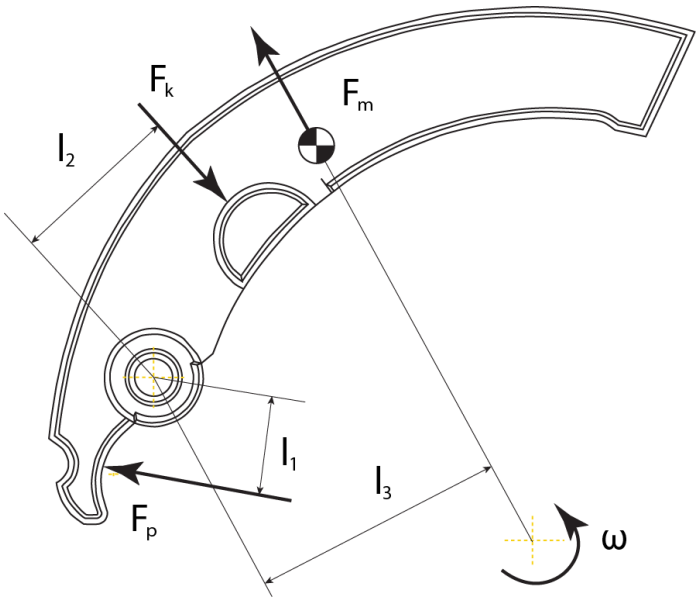

Figure 3.11 Equilibrium Equation of the lever arm.

These forces are given by

$$F_p = A_b P + m_b \omega^2 (r_b + \Delta y_1) \tag{3.28}$$

$$F_k = k_{arm} \Delta y_2 + F_c \tag{3.29}$$

$$F_m = m_{arm} \omega^2 (R_{\max} + \Delta y_3) \tag{3.30}$$

where A_b depends on the height between the outlet and the ball. To make all the equations depend on this height Δy_1, the following simplifications and relations are formed:

$$\varphi = \arcsin(\frac{\Delta y_1}{l_1}) \approx \frac{\Delta y_1}{l_1} \tag{3.31}$$

$$\Delta y_2 = l_2 \sin(\arcsin(\frac{\Delta y_1}{l_1})) \approx \frac{l_2 \Delta y_1}{l_1} \tag{3.32}$$

$$\Delta y_3 = l_3 \sin(\arcsin(\frac{\Delta y_1}{l_1})) \approx \frac{l_3 \Delta y_1}{l_1} \tag{3.33}$$

The angle and the height relations are illustrated in *Figure 3.12*. The simplification in the equations is due to the small changes in angle that will occur during operation.

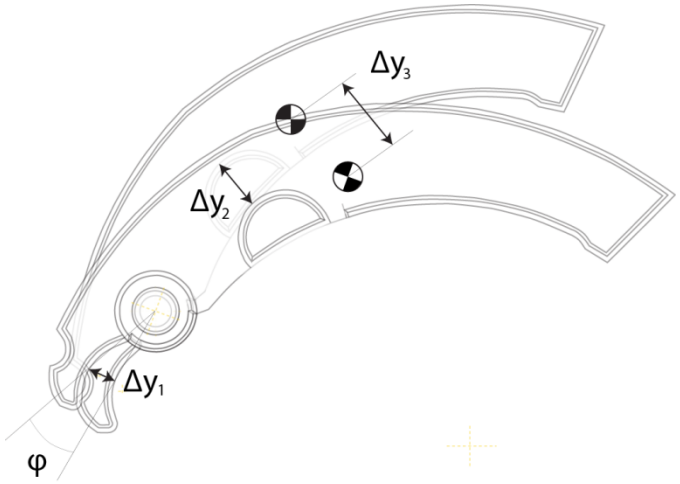

Figure 3.12 The relation between Δy_1, Δy_2 and Δy_3.

3.2.4.1 Area Function for ball

To get the force F_b the area of the ball that is subject to the oil pressure is needed. This is described by

$$A_b(\Delta y_1) = \pi \Delta y_1 (2r_b - \Delta y_1) \tag{3.34}$$

In *Figure 3.13* equation (3.34) is illustrated. The area of the ball is also used in the flow calculation.

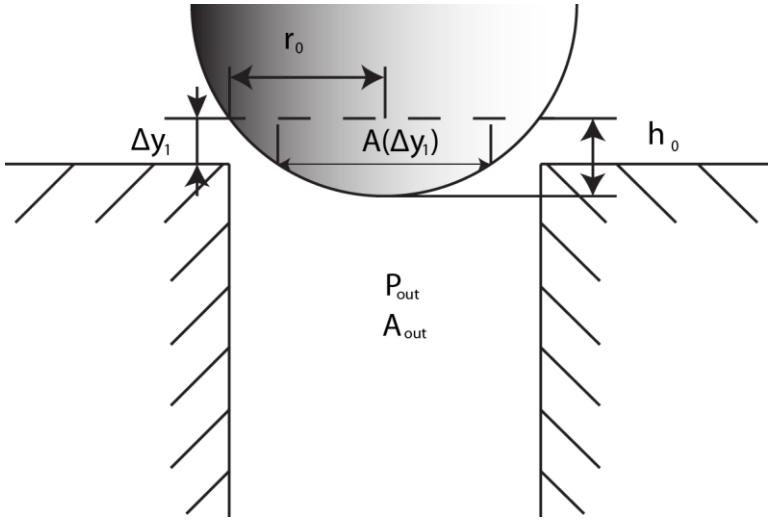

Figure 3.13 Area function for the ball as a function of Δy_1.

3.2.4.2 Hagen-Poiseuille

The Hagen-Poiseuille [7] describes the laminar flow of an incompressible fluid in a pipe. By using this flow equation the pressure drop in the channel leading to the orifice can be calculated. Assuming a known flow, *Q*, and the channel geometry, the Hagen-Poiseuille flow with our denotations become

$$Q = \frac{\pi D^4 (P_c - P)}{128 \eta L_t} \tag{3.35}$$

where η is the viscosity, D is the diameter of the pipe, L_t is the length of the pipe and P_c and P are the different pressures. This can be rearranged to

$$P = P_c - \frac{128 \eta L_t Q}{\pi D^4} \tag{3.36}$$

In *Figure 3.14* a schematic of the channel leading to the opening at the arms is shown.

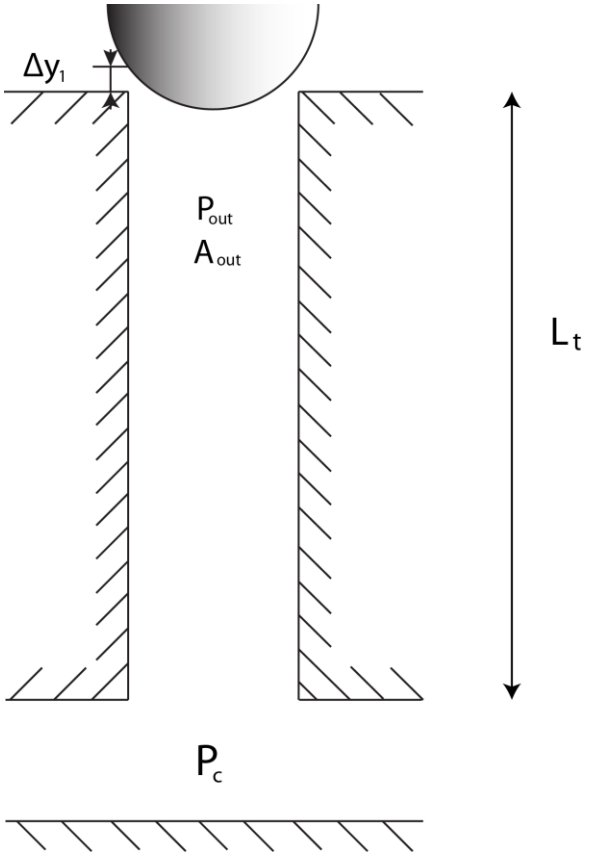

Figure 3.14 Cross-section of the discharge channel in the pump barrel.

3.2.4.3 The elevation of the ball

Δy_1 is the elevation of the ball relative to the channel orifice (see *Figure 3.11)*. By inserting (3.28), (3.29) and (3.30) into (3.27) equation (3.37) is obtained

$$(A_b P + m_b \omega^2 (r_b + \Delta y_1)) l_1 + (k_{arm} \frac{l_2 \Delta y_1}{l_1} + F_c) l_2 = m_{arm} \omega^2 (R_{\min} + \frac{l_3 \Delta y_1}{l_1}) l_3 \tag{3.37}$$

By solving this equation an expression for Δy_1 is given.

$$\Delta y_1 = -\frac{1}{2\pi l_1^{\,2} P} \left(\left(\sqrt{k_{arm}^{\,2} l_2^{\,4} - K_1 - K_2} \right) - K_3 + K_4 - K_5 + K_6 \right) - K_7 \tag{3.38}$$

$$K_1 = 2\omega^2 l_2^{\,2} m_b k_{arm}(l_1^{\,2} + l_3^{\,2} m_{arm} - \omega^2 l_1^{\,4} m_b) \tag{3.39}$$

$$K_2 = 4\pi P l_1^{\,2} l_2^{\,2}\left(r_b k_{arm} - F_{arm} l_1 \frac{1}{l_2}\right) \tag{3.40}$$

$$K_3 = 4\pi\omega^2 l_1^{\,4} m_b (r_b P + R_{\max} + P\frac{l_3^{\,2}}{l_1^{\,2} m_b} r_b m_{arm}) \tag{3.41}$$

$$K_5 = 4\pi R_{\min}\omega^2 P l_1^{\,3} l_3 m_{arm} \tag{3.42}$$

$$K_6 = \omega^4 l_3^{\,2} m_{arm}(2l_1^{\,2} m_b + l_3^{\,2} m_{arm}) \tag{3.43}$$

$$K_7 = k_{arm} l_2^2 - (l_1^2 m_b + l_3^2 m_{arm})\omega^2 + 2\pi l_1^2 r_b P \tag{3.44}$$

3.2.4.4 Flow Equation

This finally leads to the flow equation. The flow through an orifice is given by [6]

$$q_{out} = C_q A(\Delta y_1)\sqrt{\frac{2}{\rho}(P_{out} - P_{atm})} \tag{3.45}$$

$$A(\Delta y_1) = \pi r_{pipe}^2 - A_b(\Delta y_1) \tag{3.46}$$

3.2.5 Load torque to the motor

The total load torque acting on the motor shaft consists of four different torques: the viscous torque T_v, due to fluids being moved around in the pump, the friction torque in bearings and other parts moving against each other T_f, and the torque due to inertia T_I. All of these are dependent of the rotational velocity or the acceleration of the shaft.

$$m_l = T_s(\theta) + T_f(\omega) + T_I(\dot{\omega}) + T_v(\omega) \tag{3.47}$$

In *Figure 3.15* the equilibrium equation for the torque around the motor shaft is illustrated. The contribution from the piston forces to the total torque T_s, is described by

$$T_s = F_s r_1 \cos(\theta)\sin(\alpha) \tag{3.48}$$

where α is the swash plate angle and the length of the arm is described by $r_1\cos(\theta)$.

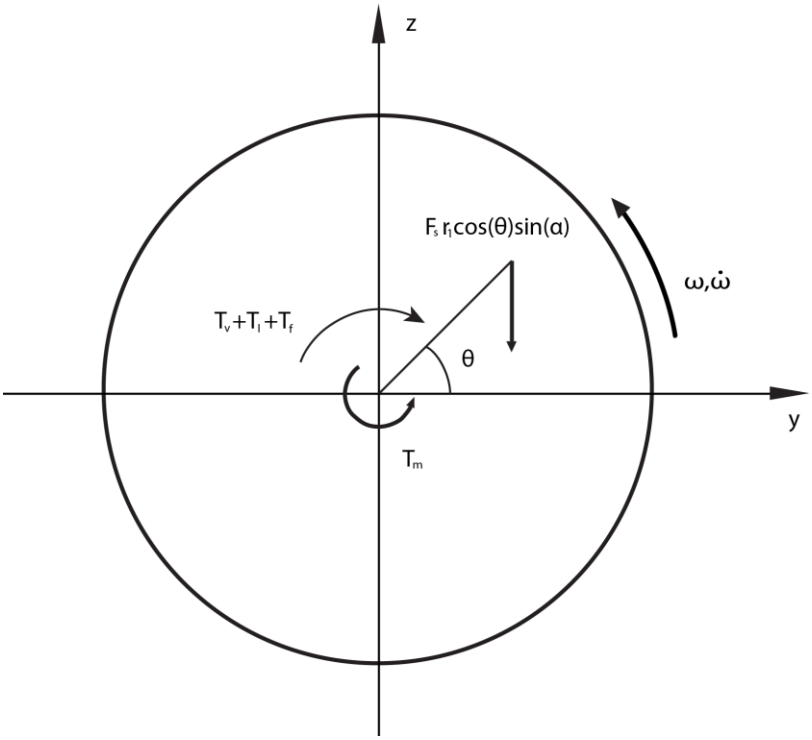

Figure 3.15 The barrel coordinates system and torques acting on it.

The friction torque in the axial thrust bearing is calculated according to the empirical relationships provided by SKF [8] and are given by

$$T_{roll} = R_1 d_m^{1.83} F_s^{0.54} (\upsilon n)^{0.6} \tag{3.49}$$

$$T_{slide} = c_{geometric} d_m^{0.05} F_s^{4/3} c_{slide} \tag{3.50}$$

$$T_f = T_{roll} + T_{slide} \tag{3.51}$$

The torque due to viscosity T_f, is, since no empirical relations for it can be found, estimated as a function of rotational velocity and acceleration. The inertia I_p, of the bearings, the barrel and the pistons were calculated using CAD system and was given a constant value. The equation for this contribution is given by

$$T_I = I_p \frac{d\omega}{dt} \tag{3.52}$$

3.2.6 Piston flow and leakages

When the barrel starts to rotate, the pistons are forced to reciprocate back and forth creating the pumping action. The ideal flow that one piston can deliver is described by equation (3.53).

$$q_{ideal} = \dot{x}_p(\theta) A_p \tag{3.53}$$

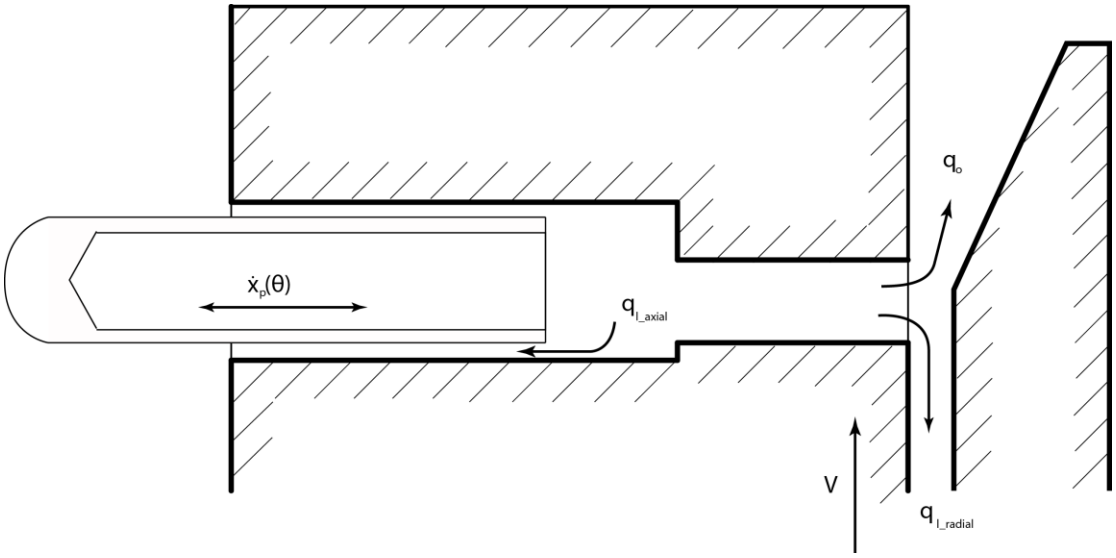

Figure 3.16 The leakage flows in the pump.

All hydraulic pumps have internal leakages. To account for these internal losses an axial direction leakage between the piston and cylinder as well as a leakage in radial direction is introduced [6]

$$q_{l\_axial} = \pi v r h_0 + \frac{\pi r h_0^3 \Delta p}{6\eta l}\left(1+1.5\left(\frac{e}{h_0}\right)^2\right) \tag{3.54}$$

$$q_{l\_radial} = \frac{\pi h^3 \Delta p}{6\eta \ln\frac{r_2}{r_1}} \tag{3.55}$$

These losses are illustrated in *Figure 3.16*. The eccentricity, *e,* of the piston is considered to be zero and therefore equation (3.54) can be simplified to (3.56)

$$q_{l\_axial} = \pi v r h_0 + \frac{\pi r h_0^3 \Delta p}{6\eta l} \tag{3.56}$$

The net pump flow can now be described by equation (3.57)

$$q_{net} = \sum_{k=1}^{6} \dot{x}_p(\theta_k) A_p - (q_{l\_axial} + q_{l\_radial})_k - q_{out} \tag{3.57}$$

3.3 The clutch pack and system pressure

There is elasticity in the pressure build up in the coupling. Different clutch packs have different elasticity depending on the actuator, the coupling housing, wear and on how many discs that is used. Therefore the clutch pack dynamics needs to be included in the model.

Haldex has performed a series of tests to establish elasticity relationships by pressurizing the clutch pack and measure the volume expansion. These measurements contain the overall characteristic including the elasticity of the oil. The elasticity data used in this simulation is based upon the characteristics of the clutch pack developed for Volkswagen.

A certain volume of hydraulic fluid in the clutch pack corresponds to a pressure level i.e. the system pressure is a function of volume. The flow is integrated over time, thereby representing a volume, and is used as an input to a look up table containing the elasticity data. The output is the system pressure, which is then fed back to the model (See Appendix A).

3.3.1 Simulink Model

The Simulink model of the pump is divided into three subsystems. First, the piston position, acceleration and speed are calculated. These are sent to the block where the load on the motor shaft is calculated as well as the block calculating the flow out of the pump. In Appendix A these blocks can be studied in further detail.

3.4 Hydraulic fluid

3.4.1 Introduction

Since the model is supposed to operate within a wide range of temperatures, the properties of the hydraulic fluid become essential. The properties to be modeled are the density, viscosity and the bulk modulus.

Since density measurements were available, the density is modeled as a function of temperature, even though hydraulic fluid can be considered as incompressible with very small density variations as a result

The viscosity has large temperature dependence and is approximated from measurements carried out at Haldex.

3.4.2 Governing equations

The properties of fluids are very complex and the physics behind are considered to lie beyond the objective for this master thesis. The mathematical model is therefore based upon empirical relationships and experimental data.

3.4.3 Density

The density is used for calculation of the dynamic viscosity. It is approximated with a linear function of the temperature.

3.4.4 Viscosity

Viscosity is a measure of the internal friction in a fluid and will affect the performance of the hydraulic pump. The kinematic viscosity, *ν*, is calculated according to the relation provided by [6]

$$\log(\log(\nu + 0.7)) = A - B\log(T_k) \tag{3.58}$$

$$A = \log(\log(\nu + 0.7)) + B\log(T_k) \tag{3.59}$$

$$B = \frac{A - \log(\log(\nu + 0.7))}{\log(T_k)} \tag{3.60}$$

By knowing the kinematic viscosity at two different temperatures, T_k, the constants A and B can be determined.

3.4.5 Bulk modulus

The bulk modulus is a measure of the fluids compressibility and is both pressure and temperature dependent. Since there was no experimental data available the bulk modulus has been modeled according to data found in Olsson O and Rydberg K-E [6], and is approximated with a quadratic function of the temperature and pressure.

3.4.6 Solution

By solving equation 3.58 the final equation for the viscosity, bulk modulus and density is derived. The constants c_1-c_4, k_1 and k_2, are used for function approximations.

$$\nu(T_k) = 10^h - 0.7 \tag{3.61}$$

$$h = \frac{10^A}{T_k^B} \tag{3.62}$$

$$\beta_t(T_k, p) = c_1 T_k^2 - c_2 T_k + c_3 + c_4 p \tag{3.63}$$

$$\eta(T_k) = \nu(T_k)\rho(T) \tag{3.64}$$

$$\rho(T) = k_1 T + k_2 \tag{3.65}$$

3.5 Complete Model

3.5.1 General Model

The complete model is, as the actual hardware, governed by the rotation of the motor shaft. Using the motor equation to solve the angle, speed and acceleration of the shaft, the axial position, speed and acceleration of each individual piston can be determined. These are then used to calculate the load torque and the flow generated by each piston. Adding these flows generates the total flow.

By subtracting the flow out through the orifice at the lever arms, the total flow in or out of the clutch is calculated. This flow is used to estimate the amount of fluid inside the clutch, which in turn is used to calculate the pressure acting on the coupling. This pressure is a deciding factor of the flow through the orifice at the lever arms and is thus fed back to this equation.

3.5.2 Simulink Model

The complete Simulink model is divided into four subsystems, the motor, pump, hydraulic fluid dynamics and one describing the pressure. The complete model is described in further detail in Appendix A.

4 Results and validation

4.1 DC-machine

The MATLAB/SIMULINK model is verified against the data provided by the manufacturer. Since there are no dynamic data available the model is only verified for static behavior with a constant voltage supply at 11 volts. In the first 24 samples the motor runs without any external load with increasing temperature from -30°C to 100°C. As seen in *Figures 4.1-4.2*, the armature current drops slightly as the temperature rises, while the rotational speed increases. This is due to reduced resistance in the coil and reduced inner frictions. The motor is then loaded with a constant torque, 20 Ncm and then the temperature is decreased back to -30 degrees.

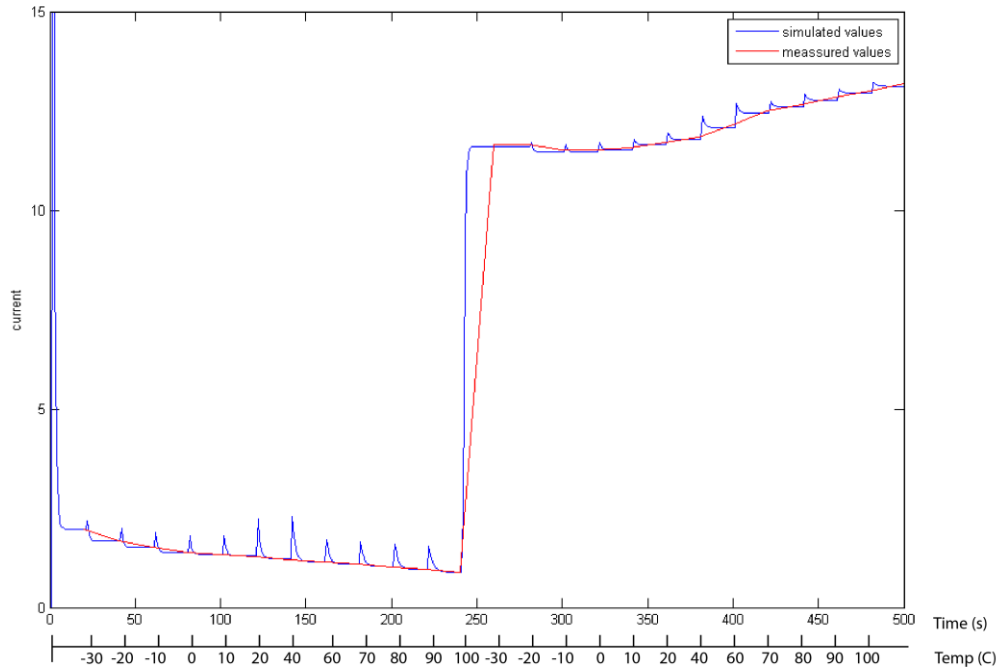

Figure 4.1 The armature current [A], in the DC-machine, first with no load from -30 to 100 degrees [C]. After 245 samples a load is applied and the temperature decreased from 100 to -30 degrees [C].

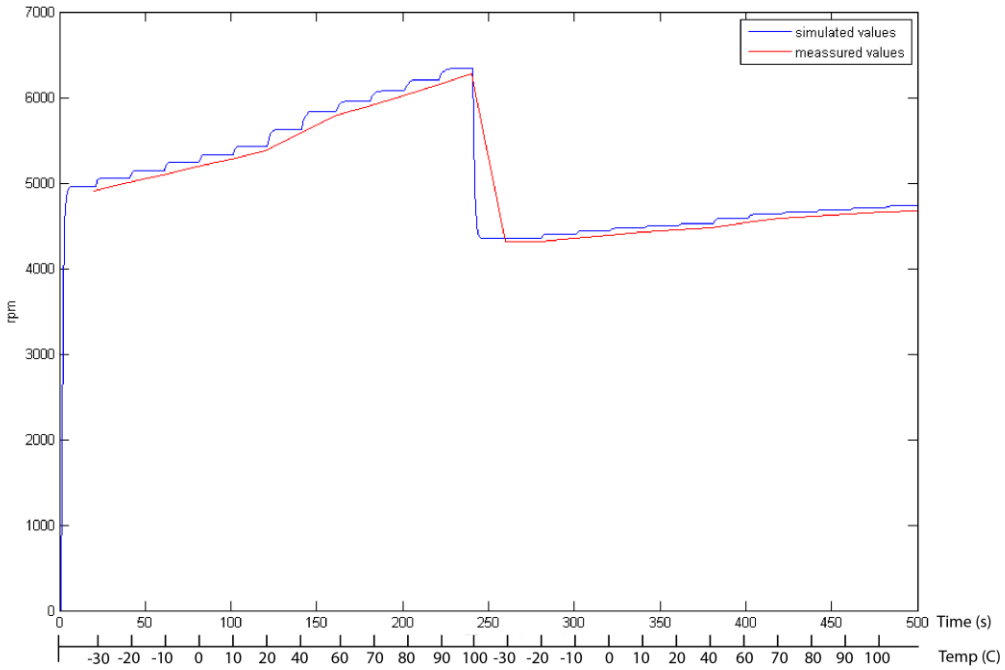

Figure 4.2 The rotational speed of the DC-machine shaft loaded and unloaded between -30 and 100 degrees [C].

The simulations show a good coherence with the figures provided by the motor manufacturer. It shall, however be mentioned that these figures, provided by the manufacturer, have a variance of 8%. Changing the motor constants will obviously have an impact on how the model performs.

4.2 Hydraulic pump

Haldex has carried out experimental measurements of the pump net flow. Although these measurements are purely static they still verify that the simulated static flows are correct.

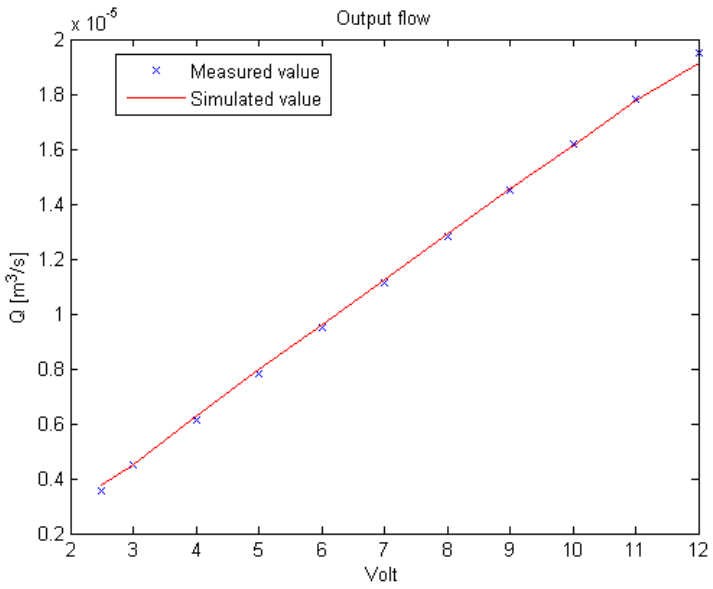

Figure 4.3 Measured and simulated static flows from the hydraulic pump.

4.3 Hydraulic fluid

The kinematic viscosity is approximated with a logarithmical function based upon measurements carried out by Haldex. The function shows good agreement with the measured values and is illustrated in *Figure 4.4*.

The density follows a linear relationship, see *Figure 4.5,* and its influence on the result is relatively small. However since measurements were available and the density is used to calculate the dynamic viscosity the function is vital.

The function for the bulk modulus is implemented in MATLAB/Simulink but is actually not used in the current model. This is mainly due to two things. When the elasticity in the LSC was introduced the compressibility of the oil was already included in the measurements. The other reason is that the hydraulic system is considered to be completely free from air mixture. The hydraulic fluid can therefore be considered as incompressible and compared to the mechanical stiffness in the LSC this would have a very small impact on the result.

However, the authors of this thesis have intentionally not removed these blocks from the model. If the circumstances change in the future they could be of use. An illustration of the modulus can be seen in *Figure 4.6.*

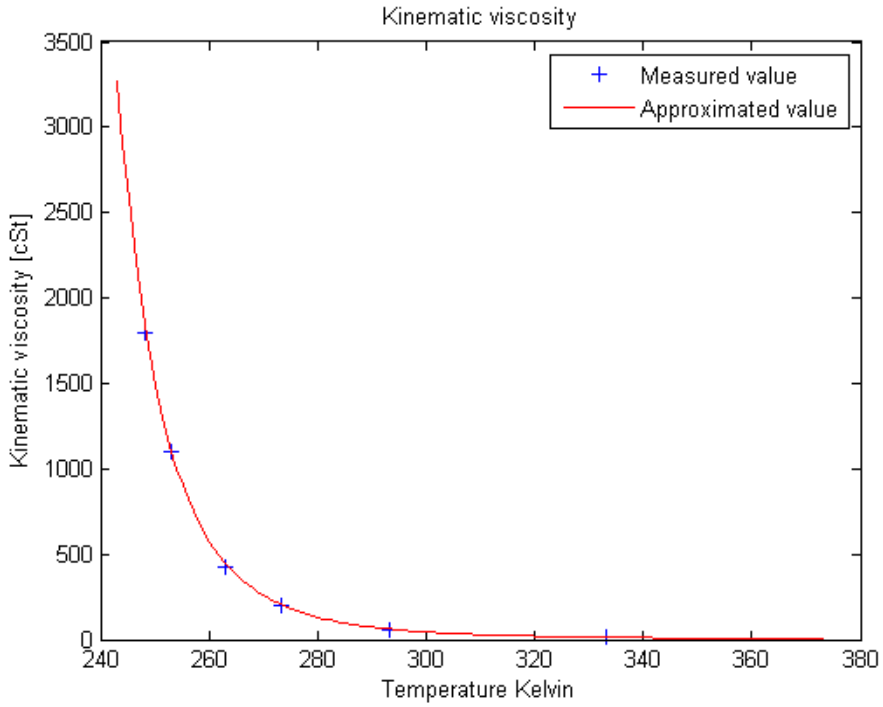

Figure 4.4The kinematic viscosity as a function of temperature.

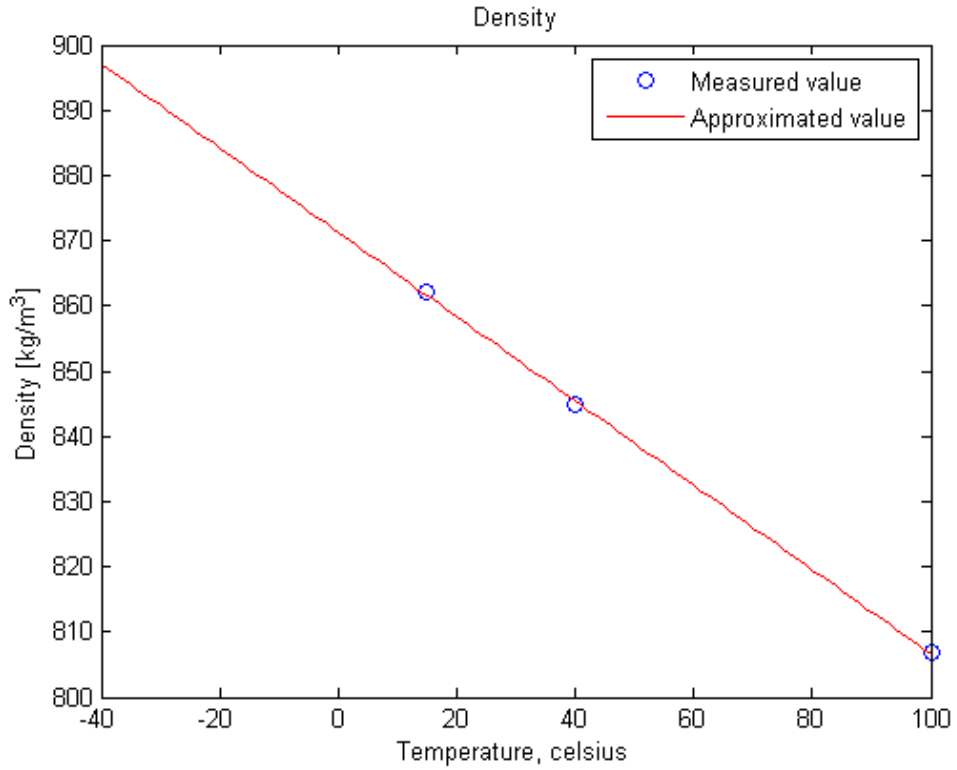

Figure 4.5 The density as a function of temperature.

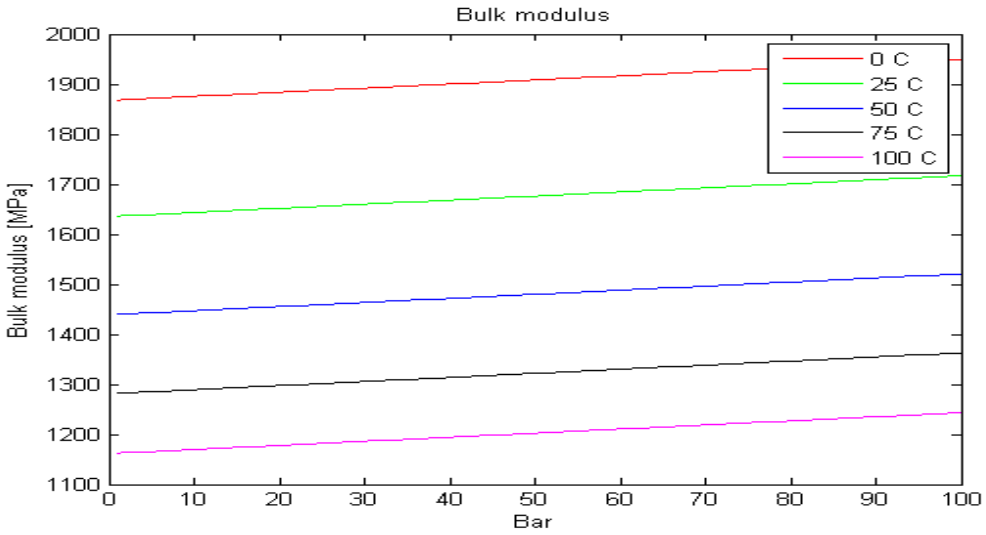

Figure 4.6 The bulk modulus as a function of temperature and pressure.

4.4 Complete Model

Measurements have been made using a test rig with the actual system. From this setup the applied voltage, resulting armature current and pressure are registered. Also the temperature of the oil and time are logged. Those data are then used for comparison with the model. Below step responses and a ramp responses are presented. Finally one session where the applied voltage is closer to an operational situation is compared to the simulation.

4.4.1 Steps

A number of steps are performed, ranging over the whole operating interval. In *Figure 4.7* the pressure of the system and model are presented. In the following figures the error between the actual pressure and the simulated is measured (*Figure 4.8*) and the difference in current is also illustrated (*Figure 4.9*).

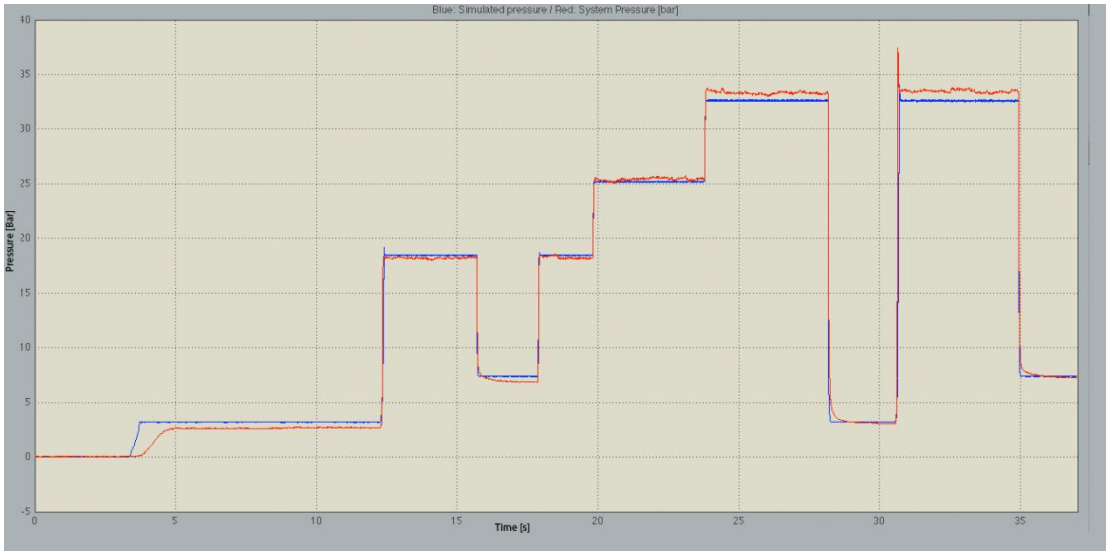

Figure 4.7 Step responses. Measured pressure (red) and simulated pressure (blue).

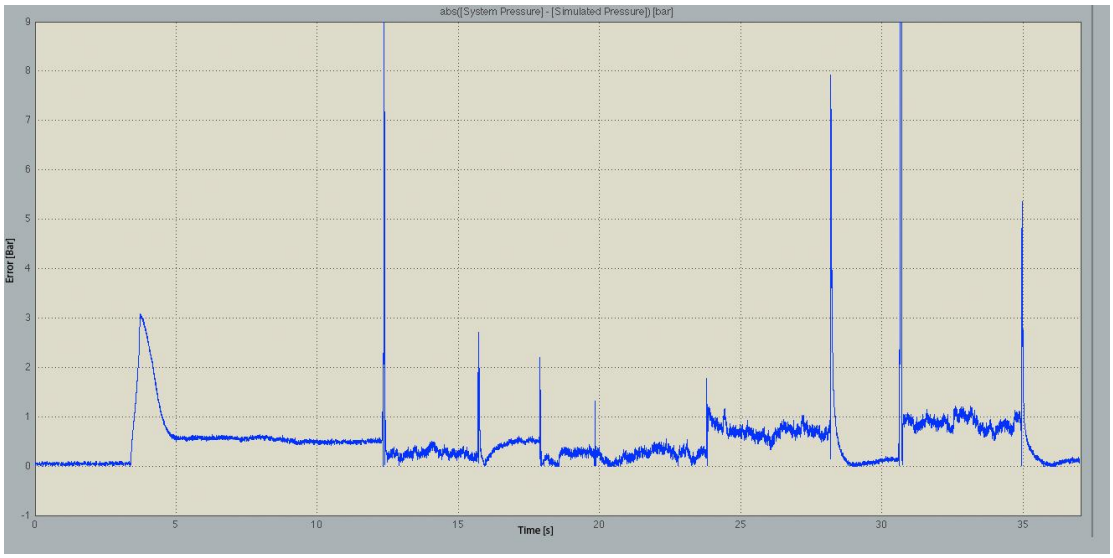

Figure 4.8 Error in pressure [bar].

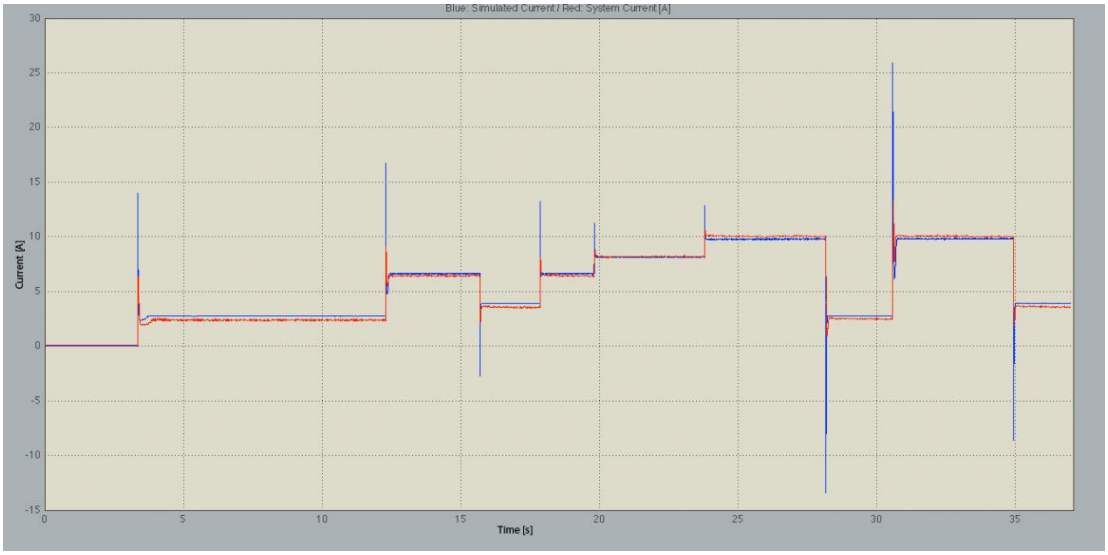

Figure 4.9 Measured current (Red) and simulated current (blue).

These comparisons show that the buildup of pressure in the simulation is somewhat fast. Although as soon as a higher pressure, above 5-7 bars is reached, the simulation closely follows the actual data. The current show the same characteristics; at lower torque and pressures the armature current is not quite following but is more accurate at higher pressures.

4.4.2 Ramp

When slowly raising and then lowering the armature voltage the system and model show the following characteristics, illustrated in *Figure 4.10* to *Figure 4.12.*

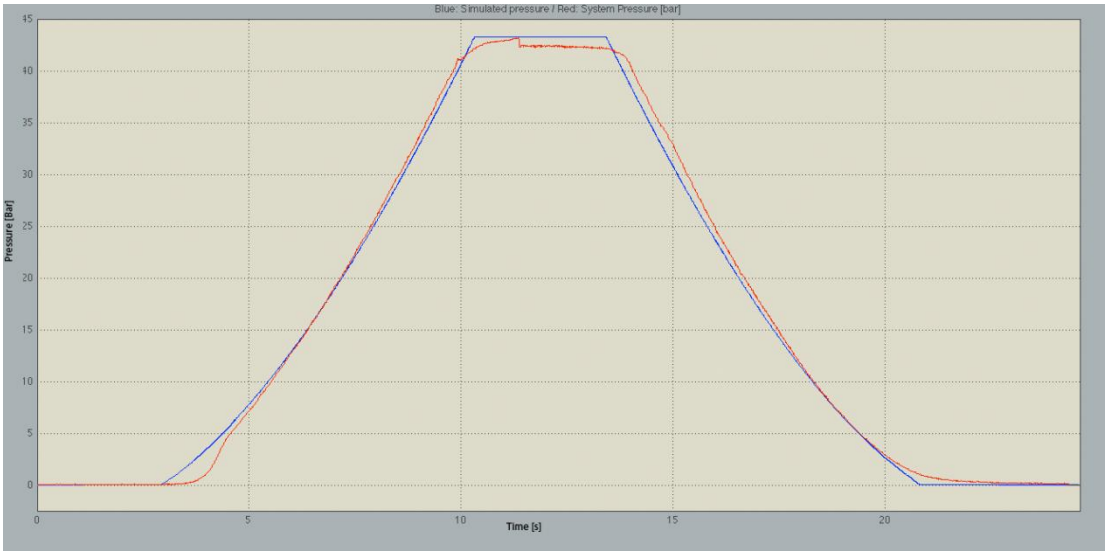

Figure 4.10 Measured pressure (red), simulated pressure (blue).

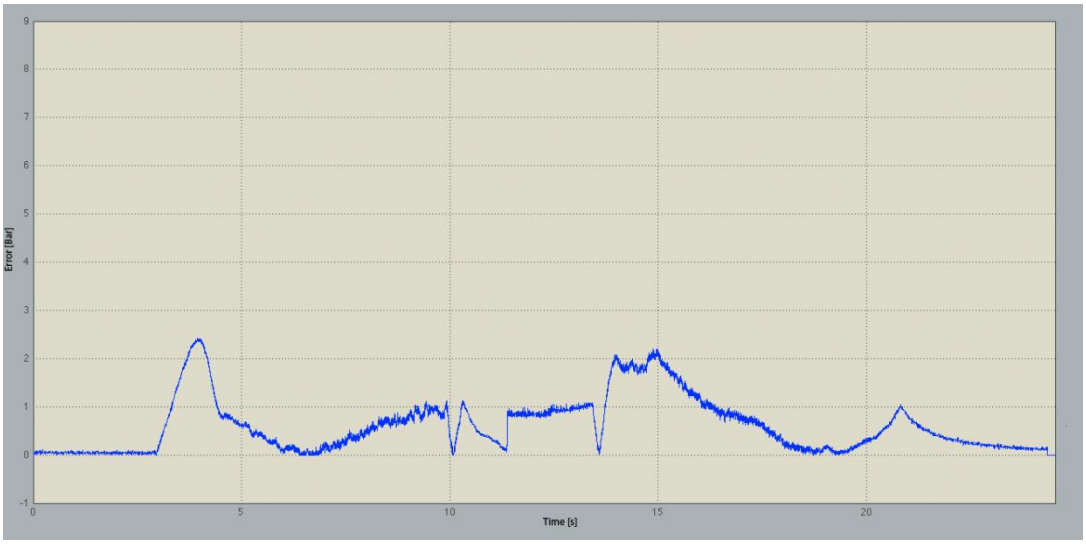

Figure 4.11 Error between actual and modeled pressure.

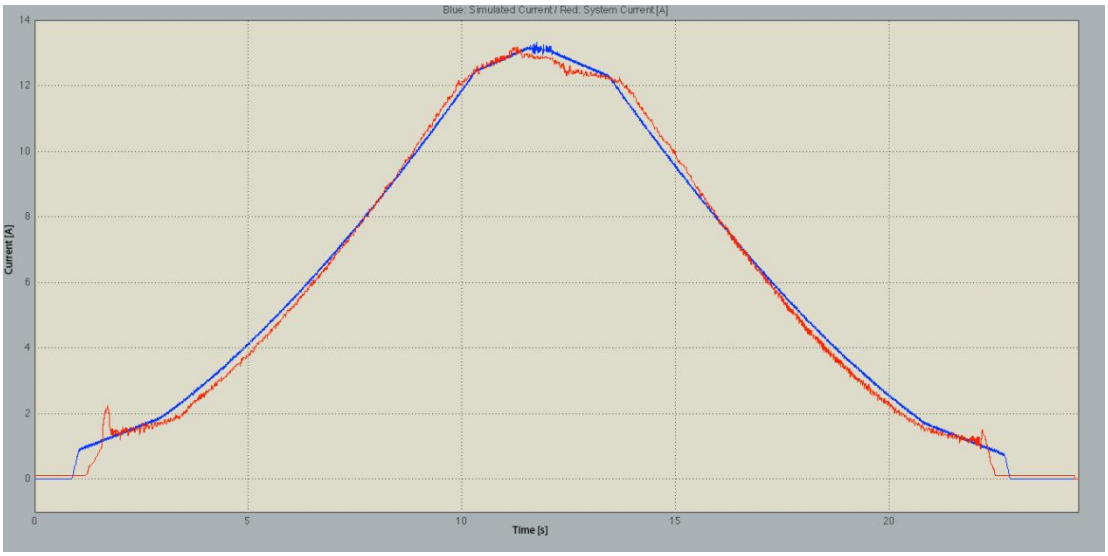

Figure 4.12 Simulated current (blue) and measured (red).

The ramp illustrates the same characteristics as the simulation with step response did. The model responds faster than the actual system. A close-up of the ramp in the interval between 2.8 to 3.8 seconds are provided in *Figure 4.13* as well as a figure illustrating the flow through the openings at the lever arms compared to the flow going out of the pump (*Figure 4.14*). There it can be seen how the flow through the orifice at the arms decrease somewhat when the pressure in the model rises. This is an irregularity compared to the rest of the ramp when the flow through the orifice follows the total flow from the pump closely, as seen in *Figure 4.15*

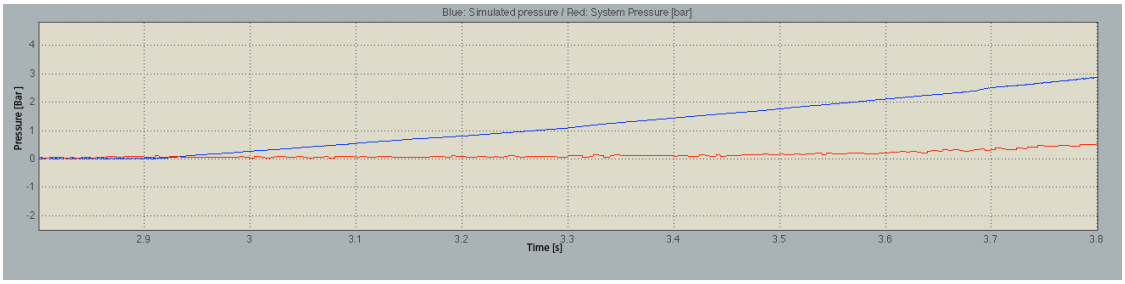

Figure 4.13 The ramp pressure as the pressure starts to rise.

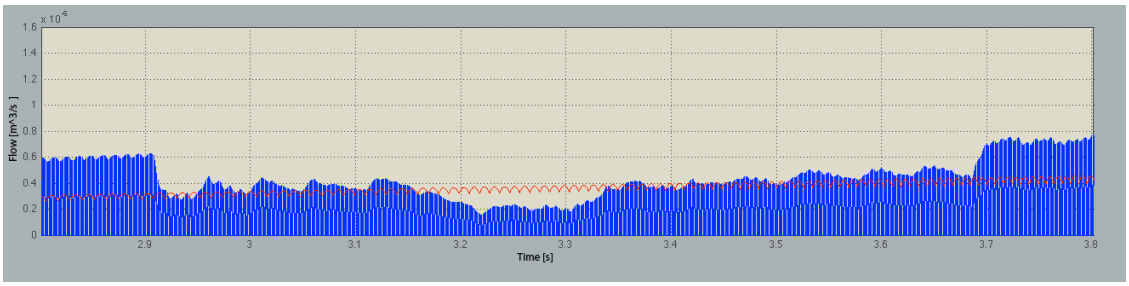

Figure 4.14 The flow from the pump (red) and the flow going out through the orifice at the lever arms (blue).

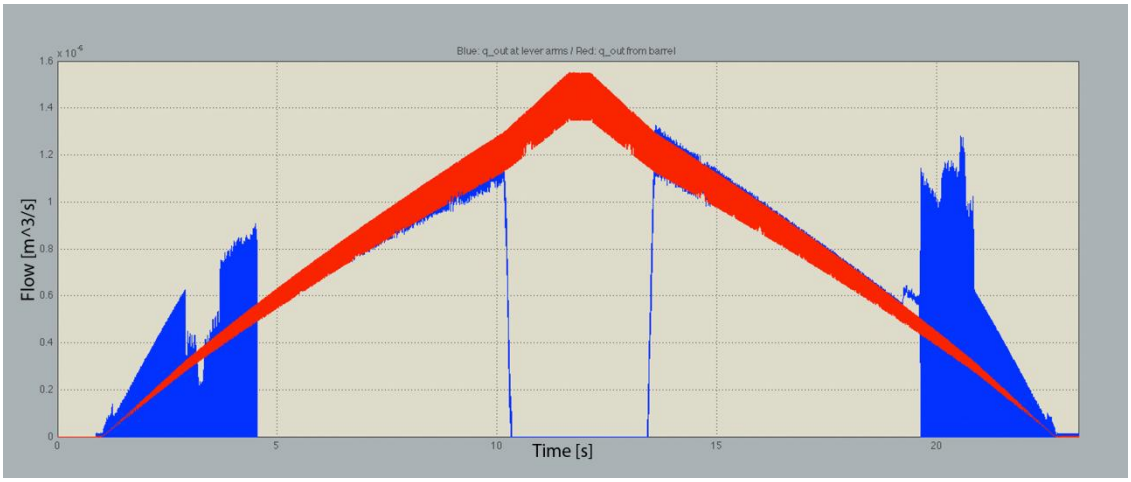

Figure 4.15 The flow from the pump (red) and the flow going out through the openings at the lever arms (blue) throughout the complete ramp cycle.

4.4.3 Operational Situation

To get an idea of how well the model follows a real operational situation a third run was performed on the rig. The objective was to mimic a situation where the car was skidding on ice or snow. By randomly changing the voltage applied to the motor in alternating high and low frequency such a situation was recorded. The pressure comparison can be viewed in *Figure 4.16.* The error (*Figure 4.17*) in pressure and the current comparisons (*Figure 4.18*) are also presented below.

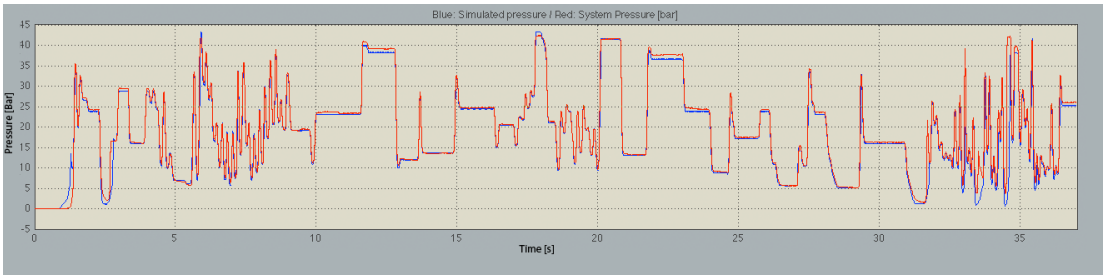

*Figure 4.16*Pressure measurements. Measured pressure (red) and simulated pressure (blue).

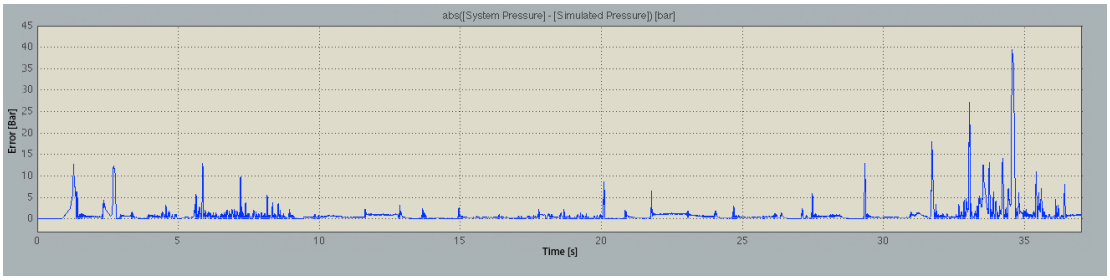

Figure 4.17 Error between measured pressure and actual pressure

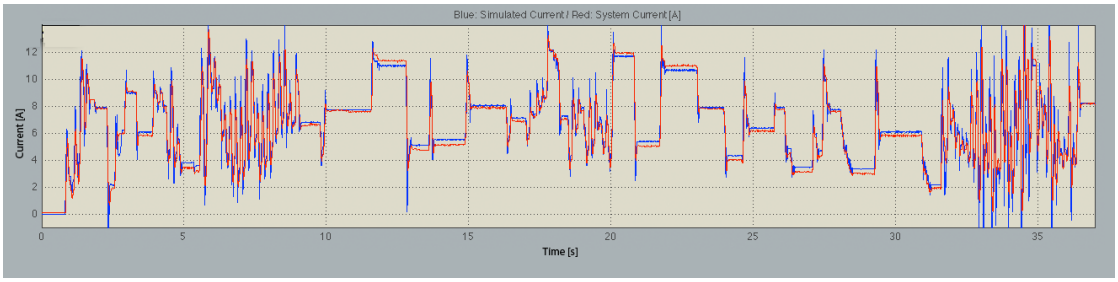

Figure 4.18 Current during operation. Measured (red) and simulated (blue).

Not surprisingly this simulation shows the same characteristics as seen in previous simulations. At low pressures, specifically at start-up, the simulation is faster than the actual system. 4.5 Error Analysis

This section will cover the accuracy of the model and by investigating and comparing the input/output of the complete model. Possible areas causing errors will also be discussed.

4.5.1 Accuracy of the Model

To determine the accuracy of the model two of the above-mentioned simulations have been studied in closer detail, the ramp and the operational situation. The error percentage between measured and simulated current and pressure was logged. The data from these simulations was sorted with regards to the armature voltage and the average error in the region of operation was calculated. The result is presented in the figures below. *Figure 4.19-4.20* shows the ramp and *Figure 4.23-4.24* shows the operational situation. The matlab code used to calculate the error can be viewed in Appendix B.

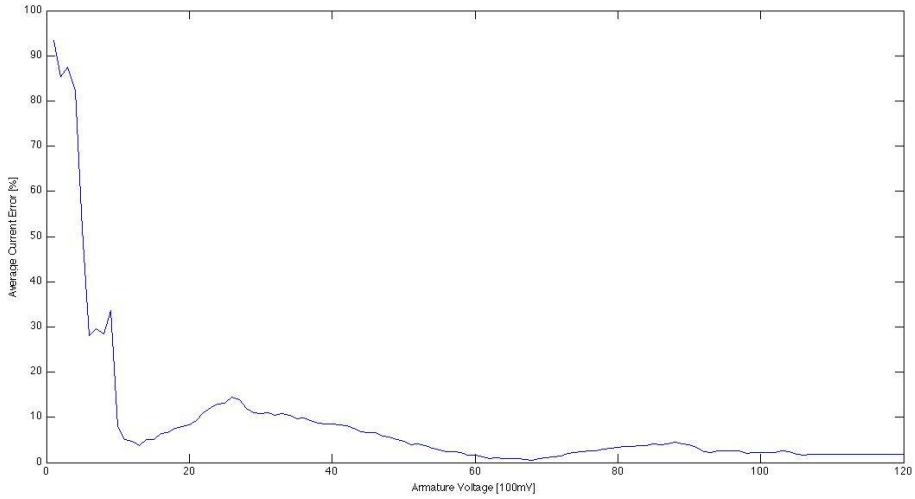

Figure 4.19 Current Error in the ramp simulation.

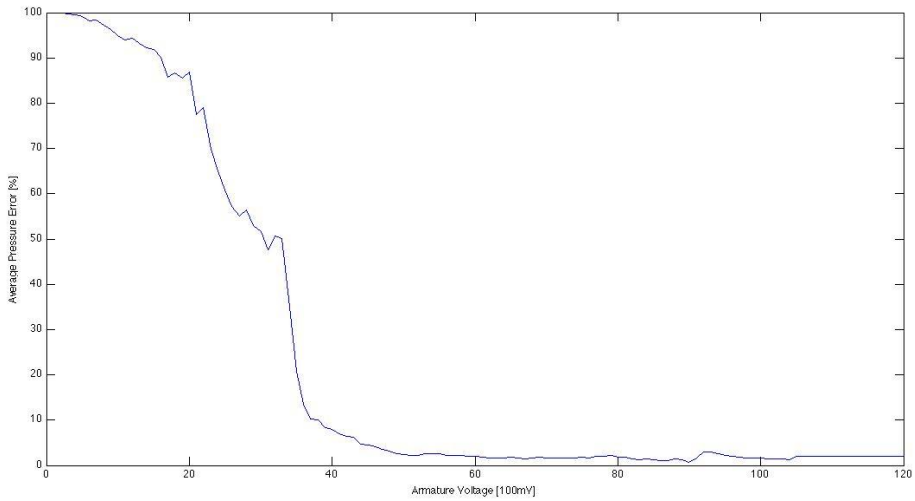

Figure 4.20 Pressure Error in the ramp simulation.

The figures above are from the ramp test cycle. As can be seen in these figures the error is larger, very large in fact, at lower voltages. This is consistent with previous results, but can be somewhat misguiding. The absolute error (see *Figure 4.11*) is very small at lower voltages, about 0.05 Bar. A closer examination of the relative error is also performed; this can be viewed in *Figure 4.21-4.22.*

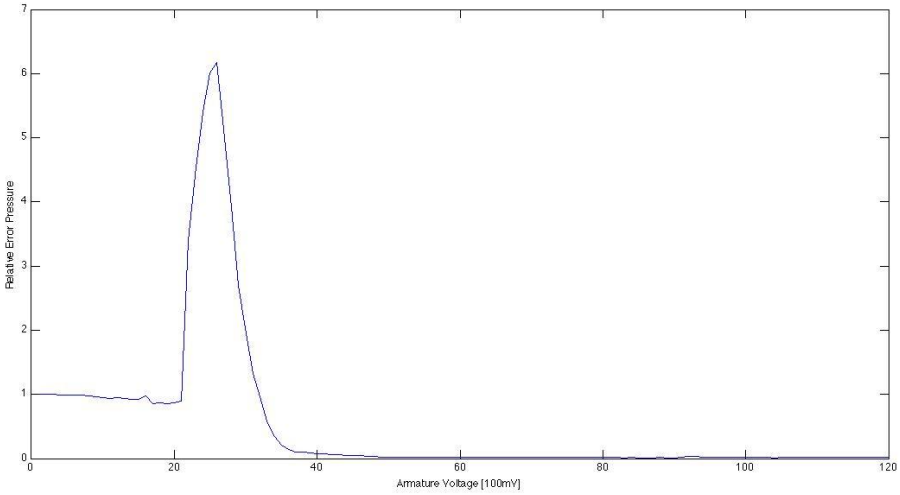

Figure 4.21. The relative error in pressure in the ramp simulation.

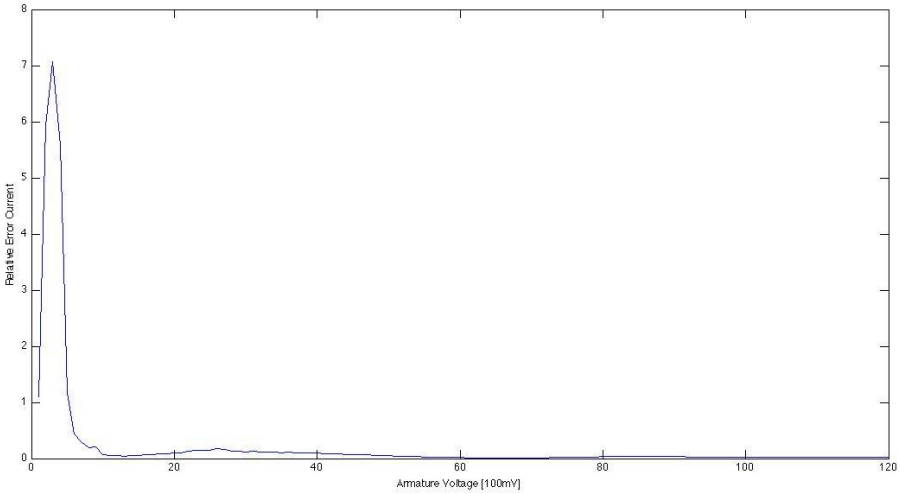

Figure 4.22 The relative error in current in the ramp simulation.

The operational situation shows a similar situation as the ramp. At lower voltages the error percentage is bigger, as well as at higher voltages. In the middle region the error is much smaller, in the following section it will be discussed why.

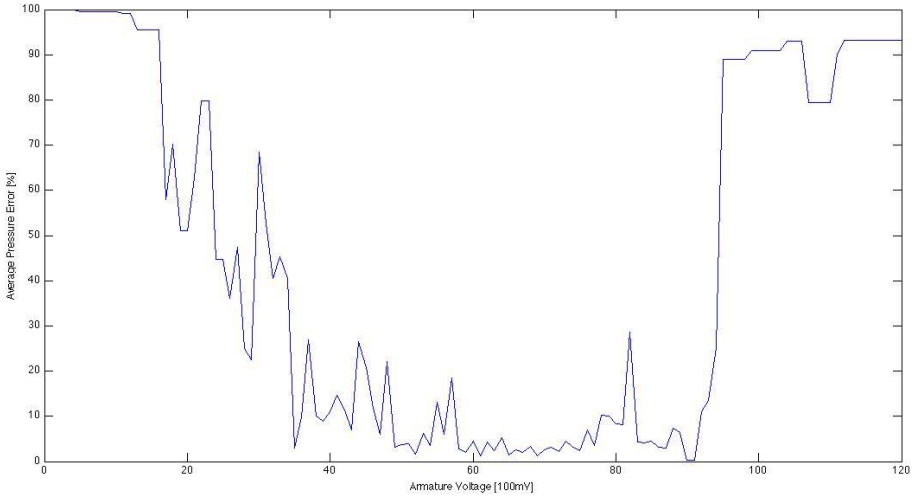

Figure 4.23 pressure error percentage during the operational situation.

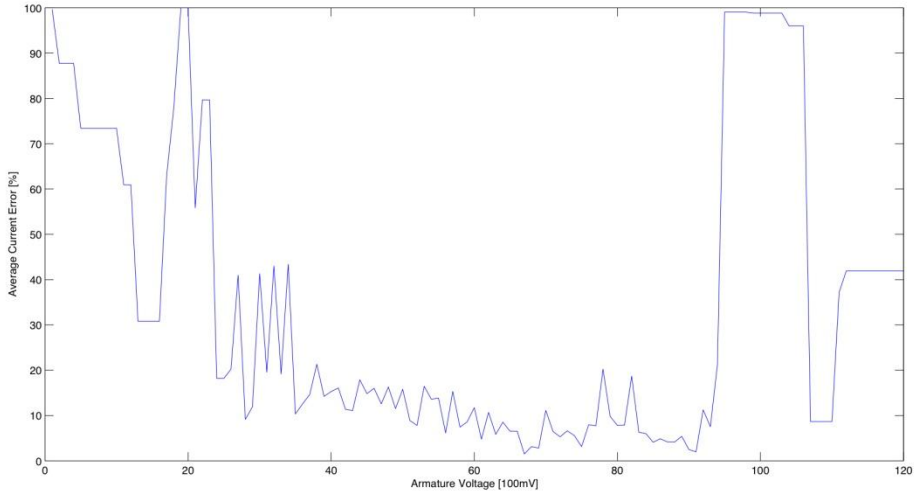

Figure 4.24 current error in percentage during operational situation.

4.5.2 Possible Causes of Error

The main reason for the big errors, percentagewise, at higher voltages, in the operational cycle, is that the voltage rarely reaches these high values during the simulation, and then only in the high frequency areas. This punishes a model that is a little slow or a little fast, creating large errors. Also, with regards to the current, large transients occur in the simulations when changes in voltage are being made. Those transients most probably occur in the real motor as well but due to a relatively slow sampling rate those will not be recorded.

Below a couple of closer examinations of the operational situation simulated results are presented.

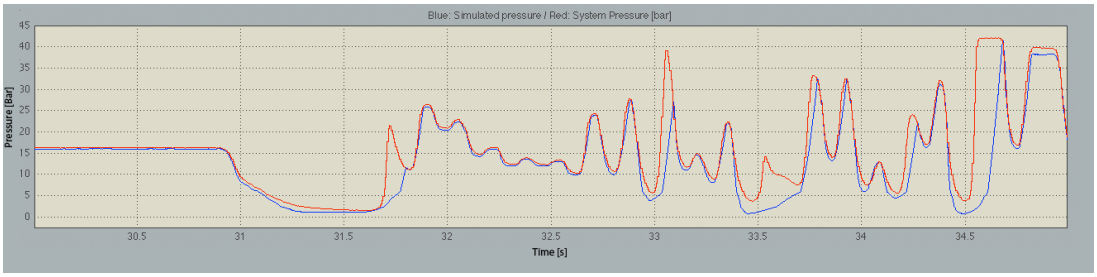

Figure 4.25 Close-up of pressure in the interval between 30 and 35 seconds.

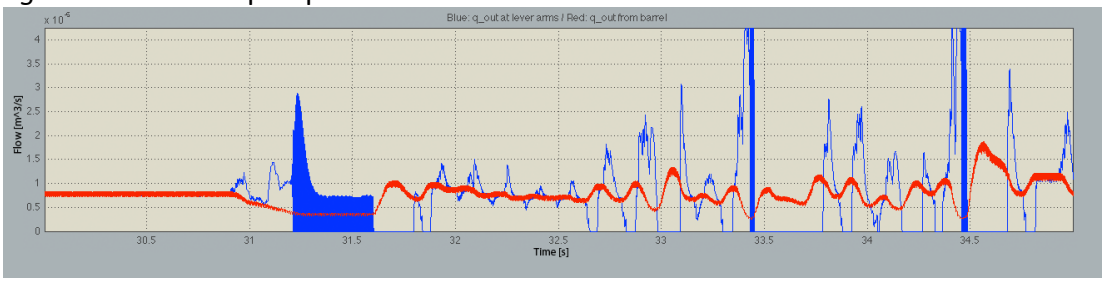

Figure 4.26 Close-up of the flows from pump and lever arms during time period 30-35 seconds of simulation.

In *Figure 4.26* the flows from the pump and the flow through the lever arms are illustrated. As seen in the ramp simulation, at low pressures the model of the flow is not perfect. The interval shown is chosen to illustrate the main weakness of the model. *Figure 4.26* highlights how the flow through the lever arm orifices at certain pressures, rotational velocities or both may not operate entirely as intended. It is speculated that this is due to equation 3.38 and the inherit instability of such an equation. Since it depends on both the pressure and the rotational velocity of the barrel and the equation has a root sign, it sometimes, in some areas has solutions in the imaginary plane. Notice the flow at 31.2-31-5 seconds where the pressure is constant but the flow through the openings is fluctuating to a high degree.

However, at a higher pressure the model follows very well the measured pressure, as seen in *Figure 4.27-4.28.*

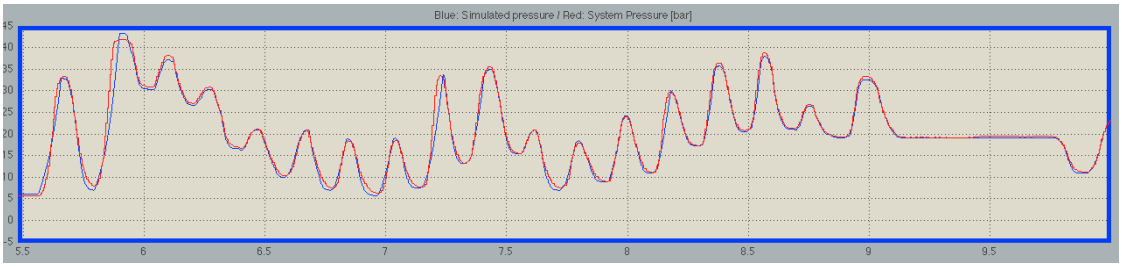

Figure 4.27 Close-up of time interval where the simulated result is good. The horizontal axis represents the time [s], the vertical axis the pressure [Bar].

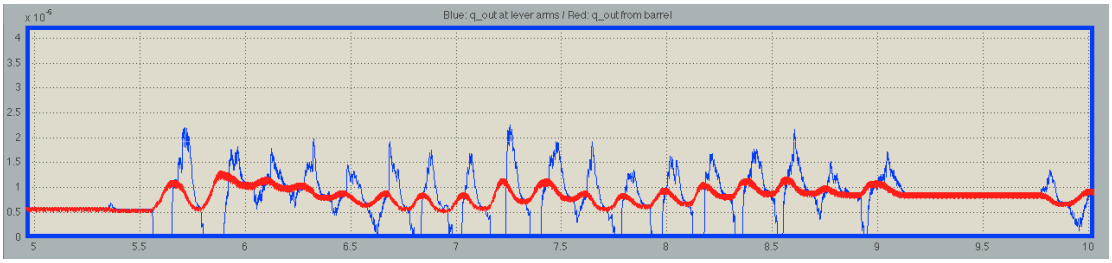

Figure 4.28 Close-up of the flows at the same interval as above. The horizontal axis represents the time [s], the vertical axis the flow [m^3/s].

This behaviour of the flow equation could be a source of error, but the elasticity function could also be contributing to errors. Since the function is based on static measurements, changes in volume of the compartment adjacent to the clutch, caused by moving parts, is not accounted for. If the volume changes so does the behaviour of the function, something that could explain the errors seen in the beginning of the ramp function (see *Figure 4.19*).

5 Conclusion

The simulation on the DC-Machine shows good coherence with the values provided by the motor manufacturer, Buhler. When considering that these motor constants have a significant variance it can be concluded that tuning these values in the model an even better result could be reached.

The simulated flows of the pump follow the measurements made by Haldex to a high degree. The temperature dependent functions for oil viscosity and density compares well with measurements made on the fluid. A function for the bulk modulus was created but later abandoned when not needed in the current model. This function has however been kept in the Simulink implementation in case of further development of the elasticity function.

Comparisons made between the complete Gen V model and the measurements from the test configuration also show good results. The step response-, ramp- and the random voltage measurements all points at the same result. When a higher pressure is reached the model follows these measurements very closely. It is when the model is building pressure from zero or a very low pressure that it differs from the tests.

It is speculated that this, too fast build up of pressure, is due to either undefined areas in the quadratic equation that governs the lever arms of the pump, errors in the elasticity function, or both.

6 Further Studies

6.1 DC-machine

The DC machine is modeled according to the standard motor equations and implemented using constants provided by the manufacturer. This model is sound and has been used in simulations for years. The model could however be further improved. Phenomena like field weakening and the influence of eddy currents could be worth investigating. Since the DC machine is the first link in the chain any flaws in this model may cause uncertainties and affecting the final result.

6.2 The Pump

Regarding the hydraulic pump there is one major component that requires more attention. The arms mounted on the barrel, which in large determines the output pressure are described by a quadratic equation with two input variables. This equation seems to be a bit unstable during certain operating conditions, at low rotational speed and low pressure, roughly up to 7 Bar. If the model needs to be more precise at lower pressures, the authors of this thesis recommend refining this function.

6.3 The Elasticity Function

This function is derived using measurements provided by Haldex. These are done in a static environment. Furthermore they are usually done on separated parts of the clutch, such as the lamellas or the piston acting on them. A better model of the elasticity could improve the model at lower pressures. This probably requires further tests and measurements on the complete clutch system.

References

[1] Haldex “Company history”. See http://www.haldex.com. Click “About us” and “company history”. Last updated: 5/4/2010. Cited: 6/10/2010

[2] Haldex “History and partners”. See http://www.haldex.com. Click “Cars”, “AWD”, “History and partners“ and “To read more about Gen I,II and III”. Last updated: 2/6/2008. Cited: 6/10/2010

[3] MathWorks “Simulink – Simulation and Model-Based Design”. See http://www.mathworks.com/products/simulink/. Click “Introduction and Key Features” and “Running a Simulation”. Last update: Not Available. Cited 10/10/2010

[4] Leonhard. W. Control of Electrical Drives. Berlin Heidelberg New York Tokyo. Springer. 1985

[5] Fitzgerald A, Kingsley C, Umas S. Electric Machinery. New York. McGraw-Hill. 2003

[6] Olsson O, Rydberg K-E. Kompendium I Hydraulik. 1993

[7] Young, Munson, Okiishi and Huebsch. A brief introduction to fluid mechanics. New York. JOHN WILEY & SONS 2007

[8] SKF Huvudkatalog 6000sv. 2006

Nomenclature

DC machine

R_a	[Ohm]	Armature resistance
L_a	[H]	Armture inductance
i_a	[A]	Armature current
e	[V]	Back EMF
u_a	[V]	Supply voltage
ω	[Rad/s]	Rotational speed
J	[kgm^2]	Rotor inertia
m_d	[Nm]	Torque generated by the motor
m_l	[Nm]	Load torque
kT	[Nm/A]	Torque constant
kE	[V/rpm]	Voltage constant
m_{fi}	[Nm]	Viscous damping
m_{tfd}	[Nm]	Dynamic friction torque
n	[rpm]	Rotations per minute
Φ_e	[Vs]	Electromagnetic flux
Ψ_m	[Vs]	Magnetic flux

Hydraulic pump

L_1	[m]	Piston length at TDC
L_2	[m]	Piston length at BDC
r_1	[m]	Radius to piston centre
x_p	[m]	Piston axial position
y_p	[m]	Piston y coordinate
z_p	[m]	Piston z coordinate
F_{t1}	[N]	Radial piston force
F_{t1}	[N]	Radial piston force
k_{arm}	[N/m]	Spring constant lever arm
k_p	[N/m]	Spring constant piston spring
F_p	[N]	Force acting on the ball
F_k	[N]	Spring force
F_m	[N]	Centrifugal force
l_1	[m]	Lever
l_2	[m]	Lever
l_3	[m]	Lever
A_b	[m^2]	Channel outlet area
P	[Pa]	Channel outlet pressure
m_b	[kg]	Ball mass
r_b	[m]	Ball radius
Δy_1	[m]	Arm displacement
Δy_2	[m]	Arm displacement
Δy_3	[m]	Arm CoG displacement

R_{min}	[m]	Minimum value for Δy_1
C_q	[-]	Flow coefficient
P_{out}	[Pa]	Channel outlet pressure
P_{atm}	[Pa]	Atmospheric pressure
r_{pipe}	[m]	Channel radius
m_p	[kg]	Piston mass
l_p	[m]	Piston length
F_s	[N]	Axial Piston force
F_f	[N]	Piston friction force
F_k	[N]	Spring force
η	[Ns/kg^2]	Dynamic viscosity
h_0	[m]	Mean clearance between piston and cylinder
P_p	[Pa]	Piston chamber pressure
A_p	[m^2]	Piston area
ΔP	[Pa]	Pressure difference
T_f	[Nm]	Opposing torque due to frictions
T_s	[Nm]	Torque due to the piston axial forces
T_l	[Nm]	Torque due to barrel inertia
I_p	[kgm^2]	Inertia of barrel and pistons
α	[rad]	Swash plate angle
T_{roll}	[Nm]	Rolling resistance in the thrust ball bearing
T_{slide}	[Nm]	Sliding resistance in the thrust ball bearing
R_1	[-]	Geometrical constant
d_m	[m]	Bearing mean diameter
υ	[m^2/s]	kinematic viscosity
$c_{geometric}$	[-]	Geometrical constant
c_{slide}	[-]	Sliding friction coefficient
β	[Pa]	Bulk modulus
q_{out}	[m^3/s]	Flow through the channels
q_{net}	[m^3/s]	Pump net flow
q_{l_axial}	[m^3/s]	Axial leakage flow
q_{l_radial}	[m^3/s]	Radial leakage flow
ρ	[kg/m^3]	Hydraulic fluid density
c_1	[m]	Piston length outside of barrel
D	[m]	Channel diameter
L_t	[m]	Channel length
Q	[m^3/s]	Flow
m_{arm}	[kg]	Lever arm mass
T_k	[K]	Temperature in Kelvin
T	[C$^\circ$]	Temperature in Kelvin

Appendix A: The Simulink Model

A.1 Complete model

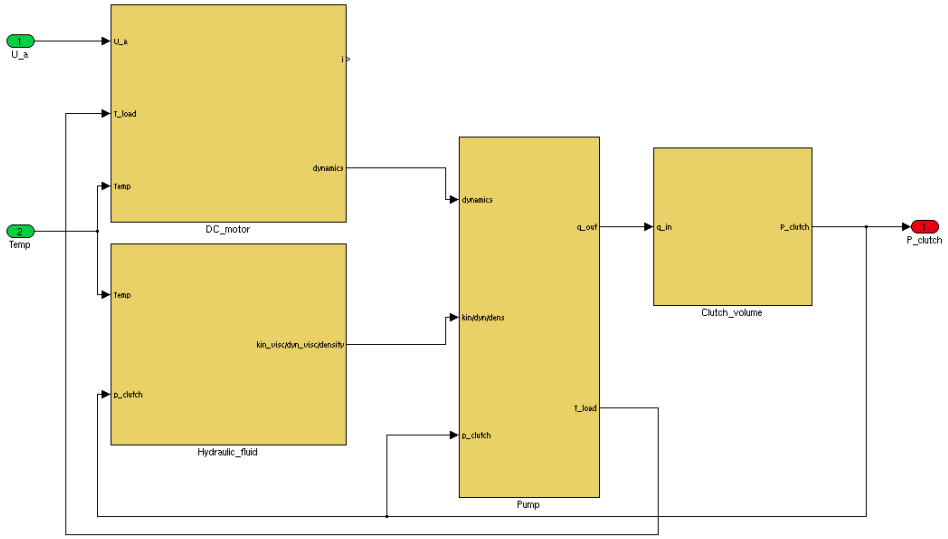

The model block contains four subsystems; the *DC_motor* block, a block calculating the dynamics of the hydraulic fluid, the *pump* block and the *clutch_volume* block.

A.2 The DC-Motor

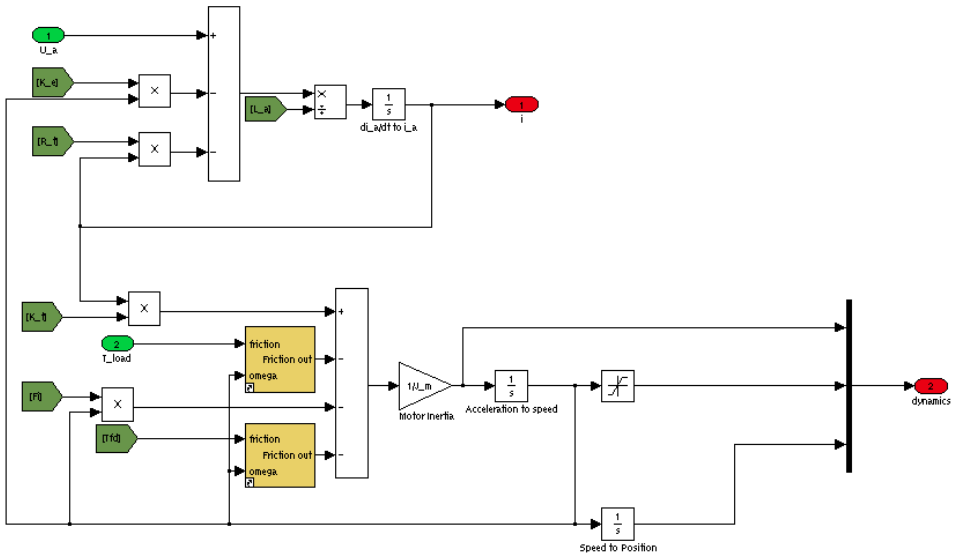

The block calculates the motor equation described in chapter 8. The input to the block is the voltage u_a, and the load torque T_load. The switches subroutines output a zero as long as the rotational velocity of the shaft is zero. This is to prevent the motor from rotating backwards at zero voltage.

A.2.1 DC-Motor Parameters

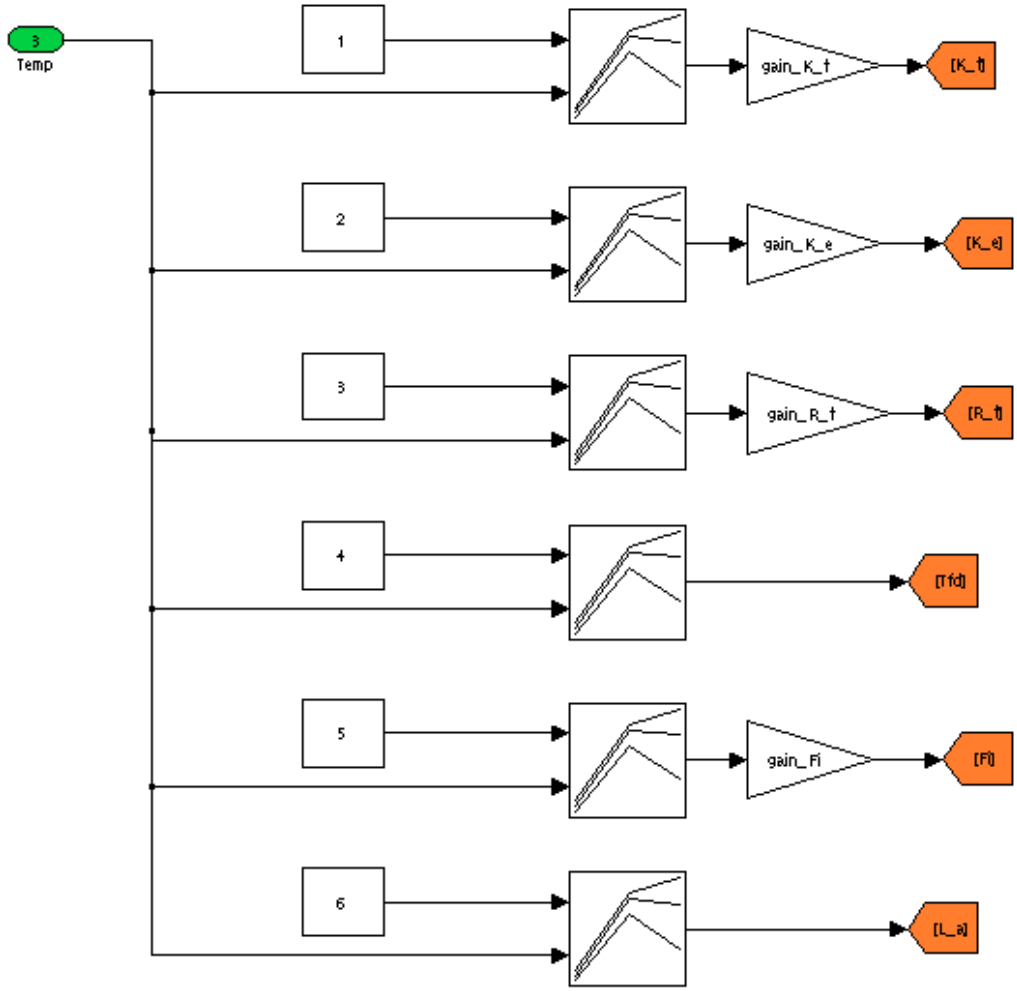

The motor parameters are contained in lookup tables. These tables are located in the *DC_motor* block and have *temp* as an input. These parameters make the motor temperature dependent. The gains on *k_t, K_e, R_t* and *Fi* are there to convert them from the provided units to S.I units.

A.3 Clutch volume

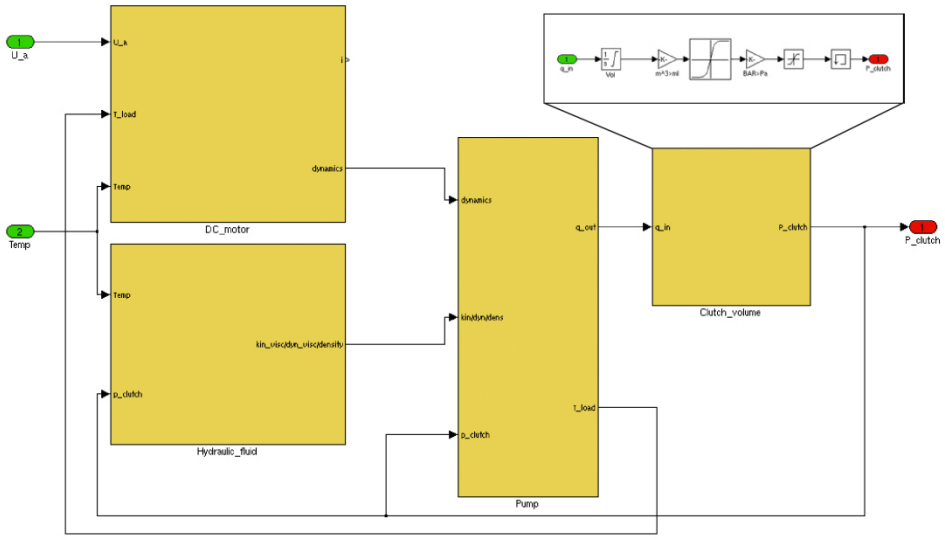

The block contains an integrator representing the volume. This is saturated to preventing it from reaching negative values. The lookup table contains the elasticity of the clutch. The output is the pressure acting on the clutch.

A.4 Hydraulic Fluid

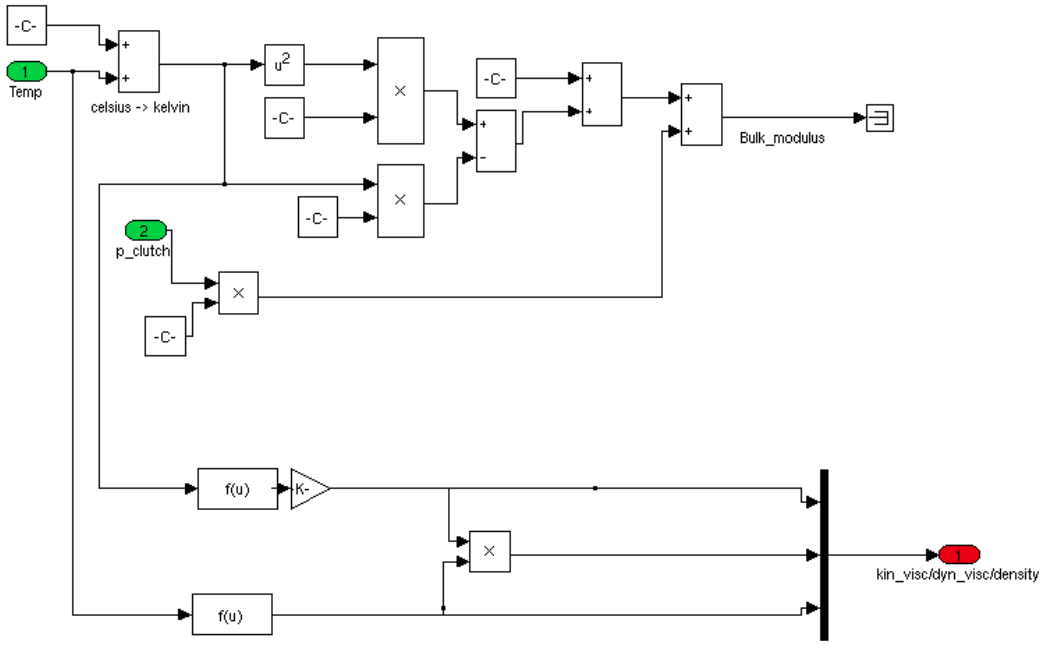

This block calculates the kinimatic- and dynamic viscosity as well as the density of the hydraulic fluid. Since these are temperature and pressure dependent *P_clutch* and *Temp* are the inputs. The *Bulk_module* is also calculated, though there is no further need for it as of now in the model and therefore that signal is terminated.

A.4 Pump

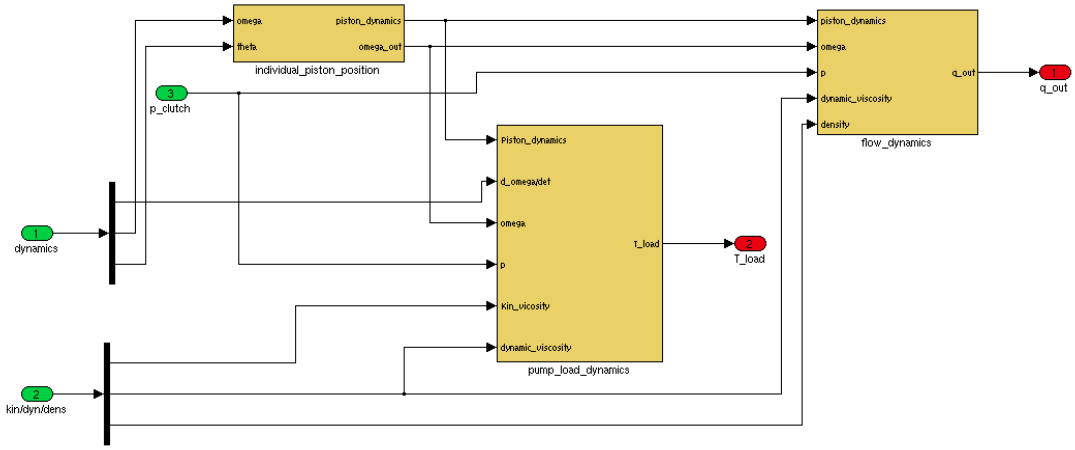

The pump is divided into tree subsystems. The *individual_piston_position* block decides the position, speed and acceleration for each piston sending these out in an array called *piston_dynamics*. The *pump_load_dynamics* block calculates the load on the motor shaft. Finally, the *flow_dynamics* block represent the flow going into or out of the volume next to the clutch piston.

A.4.1 Induvidual Piston Position

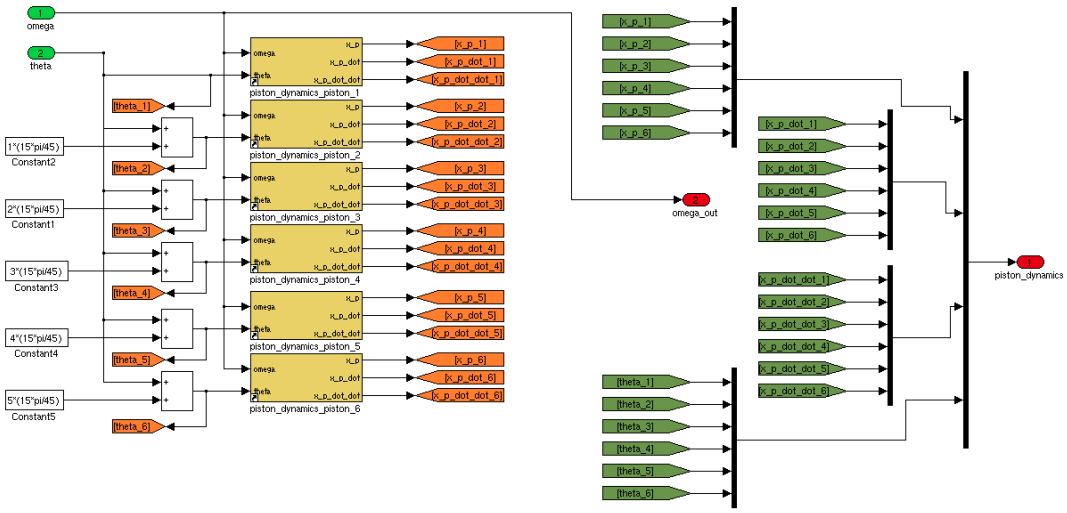

This block calculates the position, speed and acceleration for each of the six pistons.

A.4.2 Piston Dynamics

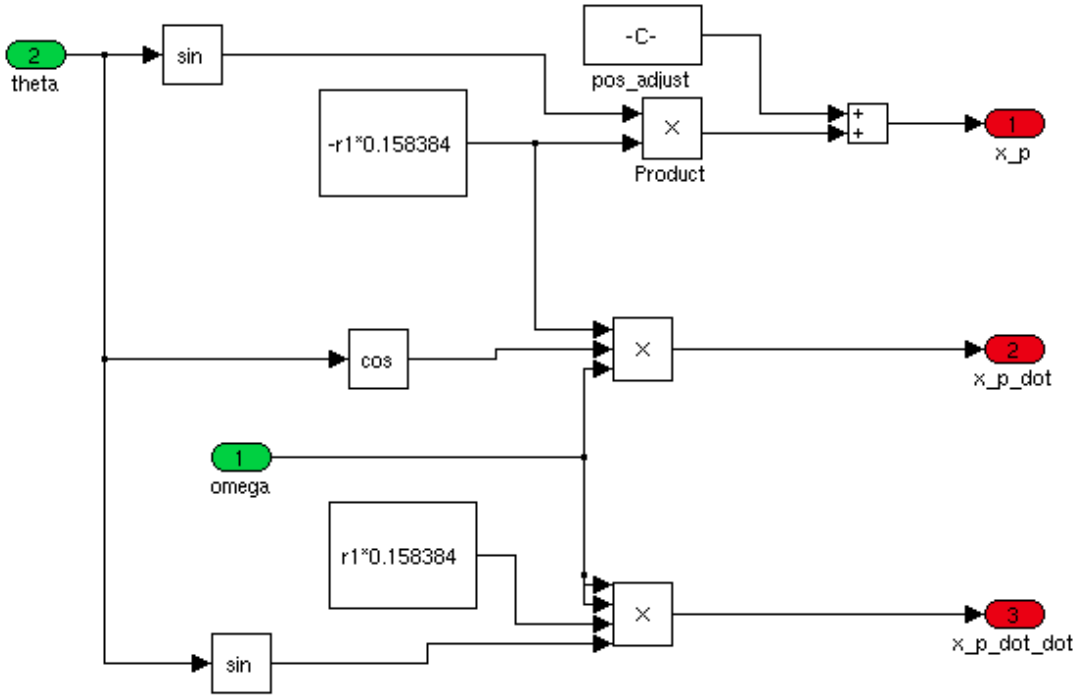

In this subsystem the piston position, speed and acceleration are calculated. The constant *pos_adjust* is there to balance the equation for the position, so that the result always is positive.

A.4.3 Piston Load Dynamics

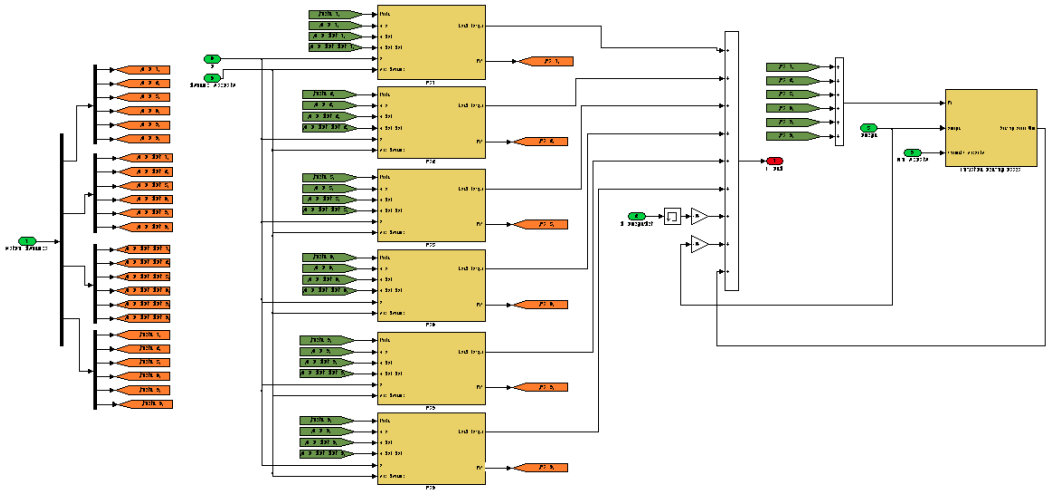

In this block the piston forces for each piston are calculated. These forces are then used to calculate the load torque acting on the motor shaft. This is partly calculated in the same blocks calculating the forces, but the bearing losses and friction losses are calculated separately. This is because the bearing losses are dependent of the sum of all the piston forces.

A.4.4 Fs (Force on the Swash plate)

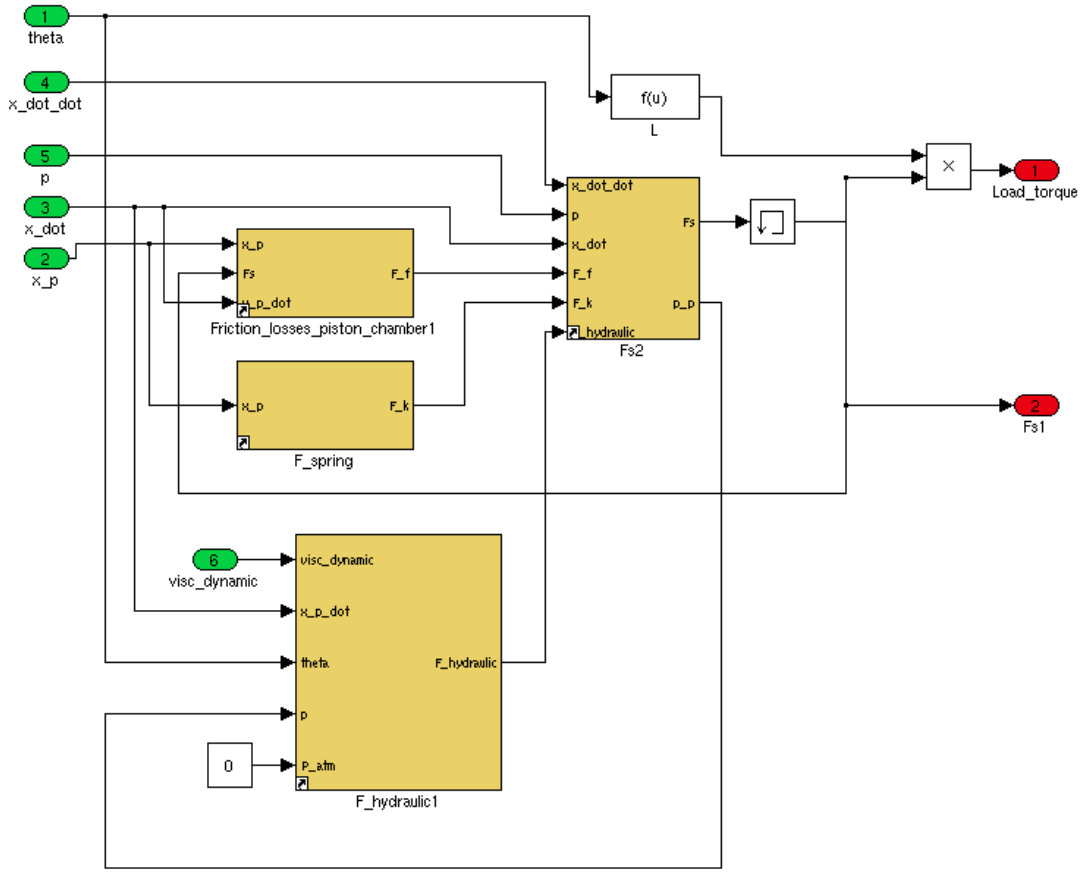

This block calculates the force F_s, the force from the piston acting on the swashplate. The block also calculates the load torque this force results in. F_s also decides the bearing losses and is thus sent out of the block to be used in further calculations. The load torque is the sum of the spring force, friction losses and hydraulic losses multiplied by the lever, L. The subsystem Fs2 sums these losses and forces. The function L calculates the lever.

A.4.5 Flow dynamics

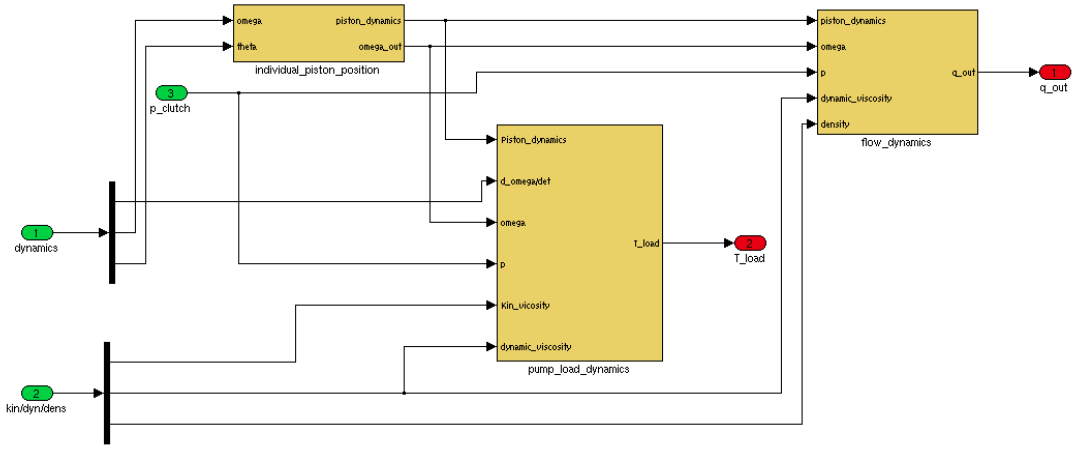

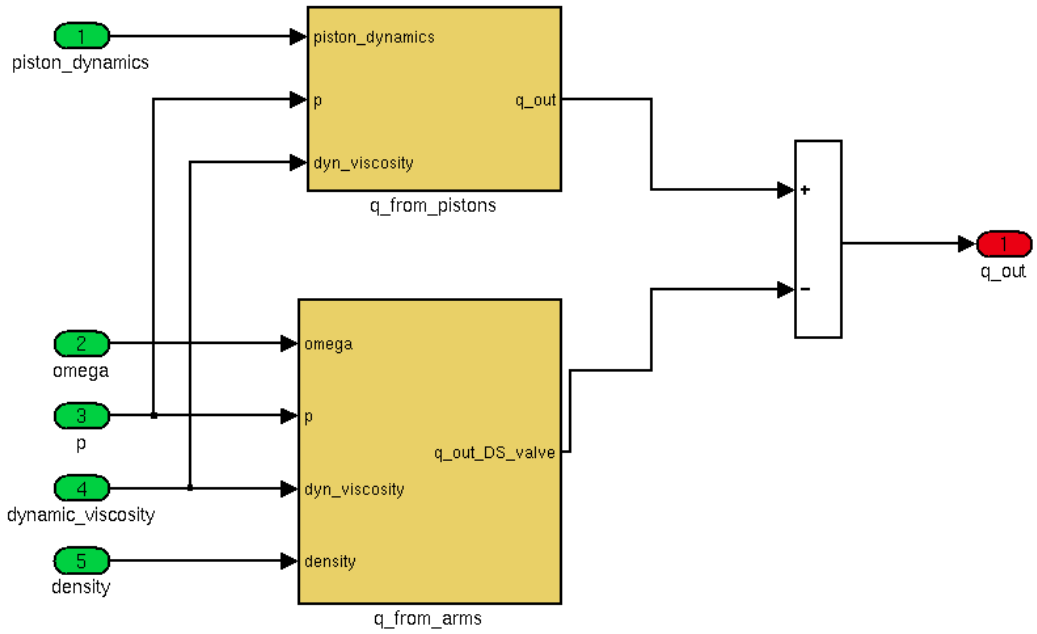

The block describes the sum of the flows going into and out of the clutch chamber. A positive *q_out* can be interpreted as the volume most adjacent to the clutch piston. A negative value can be interpreted as if the flow from the pistons as well as the clutch chamber volume is going out through the lever orifice. This flow is the input to the block in Appendix A.3 Clutch Volume.

A.4.6 Flow from the barrel and leak flow

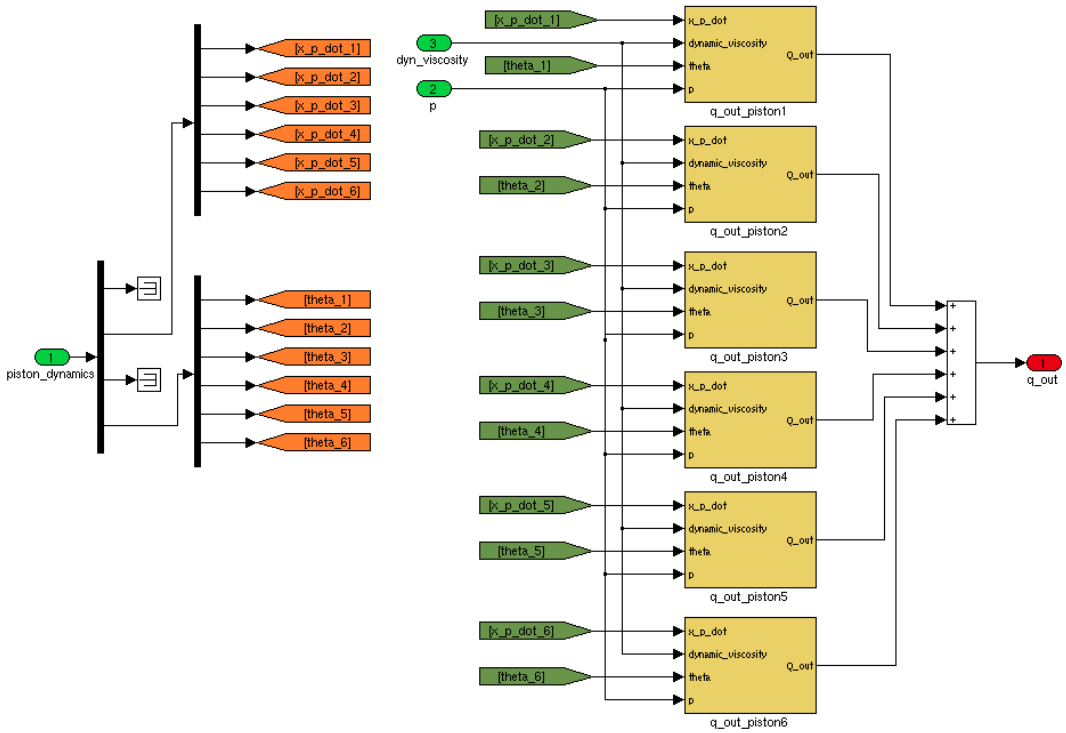

The positive flow, i.e. the flow going *out* of each piston chamber is added together generating the total sum of all these flow.

A.4.7 Flow from single piston

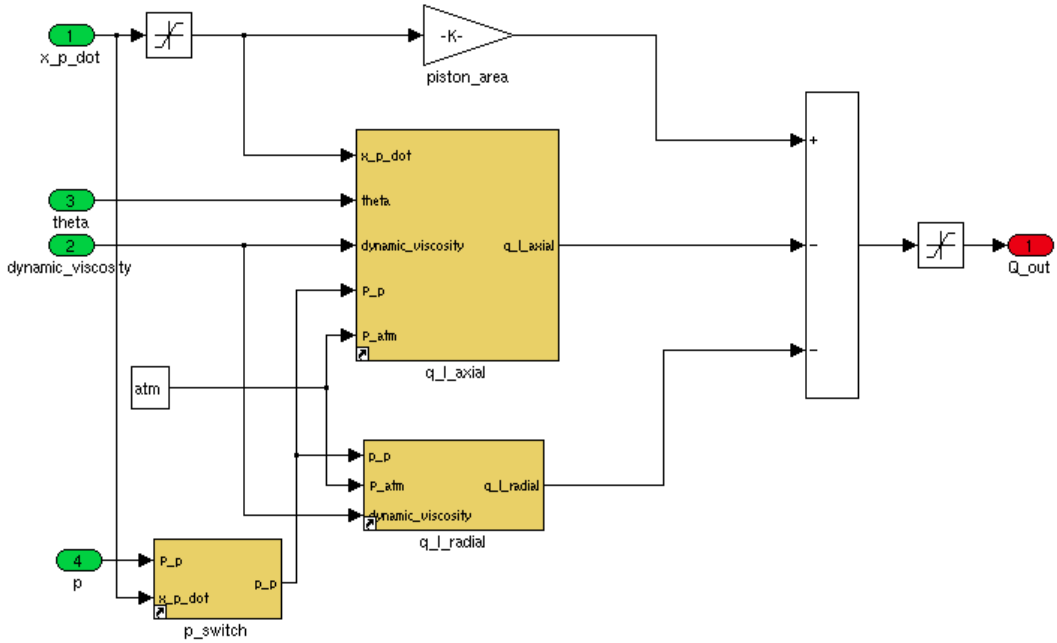

This block describes the outgoing flow from one piston chamber through the high-pressure side. The flow equation takes the piston area, multiplies it with the positive speed of the piston generating the flow. This is subtracted by the leak flows. The p_switch block simply switches the pressure in the chamber according to where the piston is located, high- or low-pressure side.

A.4.8 Flow from the discharge valves/levers

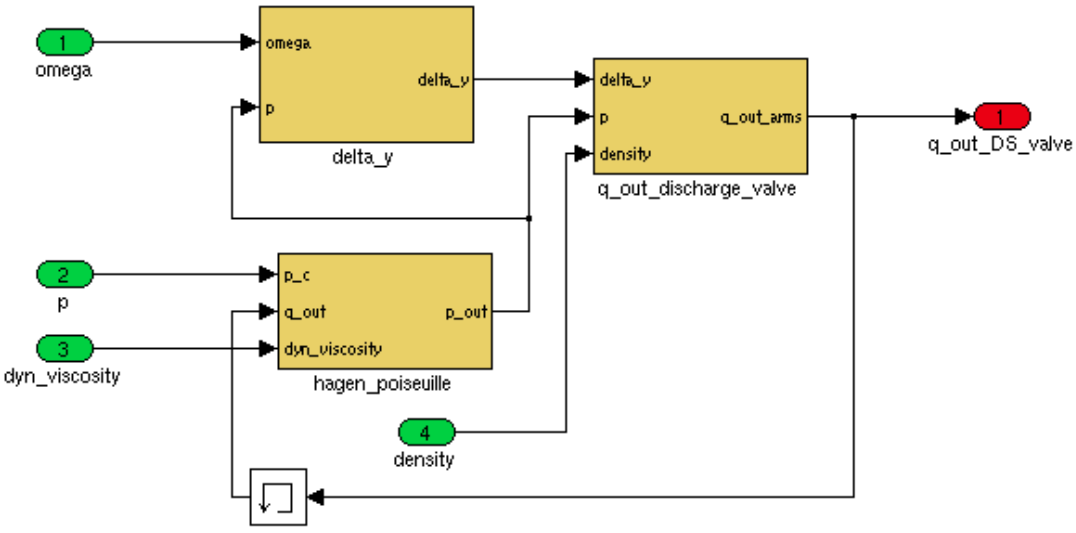

These blocks are together calculating the flow out through the orifices at the levers. This is described in more detail below.

A.4.9 Hagen-Poiseuille pressure loss

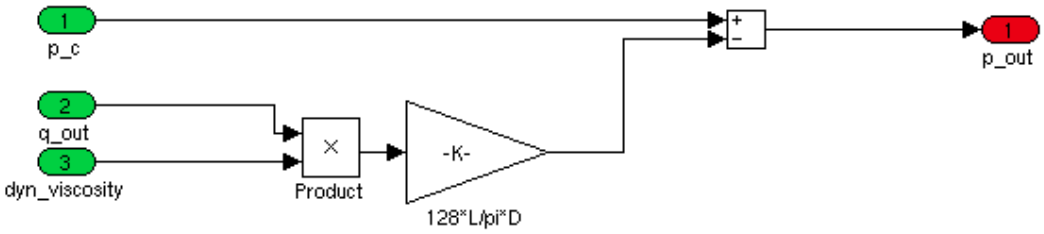

Describing the loss in a channel, the Hagen-Poiseuille equation is illustrated above. The incoming signal p_c is the pressure in the clutch volume. The outgoing signal is the pressure acting on the ball connected to the lever.

A.4.10 Delta y

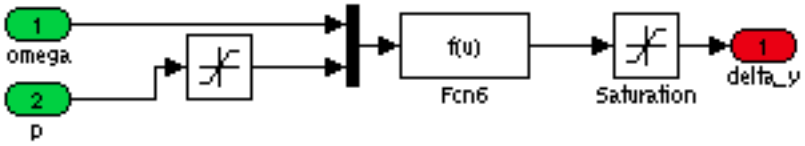

This function block determines the elevation of the lever. The incoming pressure is saturated, preventing it from becoming negative. This is because the previously described Hagen-Poiseuille losses block will, if the clutch volume pressure is zero, force the pressure to reach negative values, which is unrealistic.

A.4.11 Flow out from discharge valves

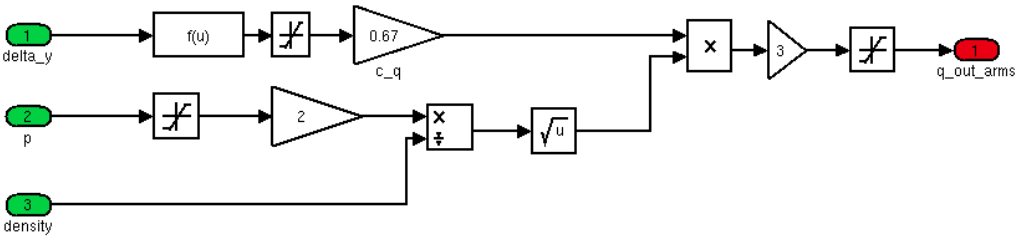

This is the equation describing the flow through an orifice. The function block at the top of the model calculates the area of this orifice. The flow is multiplied by three, since that is the number of orifices, thus resulting in the total flow.

Appendix B: Matlab Code

```
%script used to calculate the average error [%] with
%regards to voltage
%Error_analysis is a matris with dimensions [70001x4]
%and contains the data:
%[voltage(n) Pressure(n) absolute_error(n) Current(n)]


P=zeros(1,120);
C=zeros(1,120);
for k=1:120
    j=0;

    for i=1:70001


       if Error_analysis(i,1)>=(k/10-0.1) &&
Error_analysis(i,1)<(k/10)
            P(k)=P(k)+Error_analysis(i,2);
            C(k)=C(k)+Error_analysis(i,4);
            j=j+1;
       end
    end
        if j>0
            P(k)=P(k)/j;
            C(k)=C(k)/j;
        else if k>1
            P(k)=P(k-1);
            C(k)=C(k-1);
        end
        end


end
```